

---

# Multimodal Deep Learning

---

Jiquan Ngiam<sup>1</sup>  
Aditya Khosla<sup>1</sup>  
Mingyu Kim<sup>1</sup>  
Juhan Nam<sup>1</sup>  
Honglak Lee<sup>2</sup>  
Andrew Y. Ng<sup>1</sup>

JNGIAM@CS.STANFORD.EDU  
ADITYA86@CS.STANFORD.EDU  
MINKYU89@CS.STANFORD.EDU  
JUHAN@CCRMA.STANFORD.EDU  
HONGLAK@EECS.UMICH.EDU  
ANG@CS.STANFORD.EDU

<sup>1</sup> Computer Science Department, Stanford University, Stanford, CA 94305, USA

<sup>2</sup> Computer Science and Engineering Division, University of Michigan, Ann Arbor, MI 48109, USA

## Abstract

Deep networks have been successfully applied to unsupervised feature learning for single modalities (e.g., text, images or audio). In this work, we propose a novel application of deep networks to learn features over multiple modalities. We present a series of tasks for multimodal learning and show how to train deep networks that learn features to address these tasks. In particular, we demonstrate cross modality feature learning, where better features for one modality (e.g., video) can be learned if multiple modalities (e.g., audio and video) are present at feature learning time. Furthermore, we show how to learn a shared representation between modalities and evaluate it on a unique task, where the classifier is trained with audio-only data but tested with video-only data and vice-versa. Our models are validated on the CUAVE and AVLetters datasets on audio-visual speech classification, demonstrating best published visual speech classification on AVLetters and effective shared representation learning.

## 1. Introduction

In speech recognition, humans are known to integrate audio-visual information in order to understand speech. This was first exemplified in the McGurk effect (McGurk & MacDonald, 1976) where a visual /ga/ with a voiced /ba/ is perceived as /da/ by most subjects. In particular, the visual modality provides infor-

mation on the place of articulation and muscle movements (Summerfield, 1992) which can often help to disambiguate between speech with similar acoustics (e.g., the unvoiced consonants /p/ and /k/).

Multimodal learning involves relating information from multiple sources. For example, images and 3-d depth scans are correlated at first-order as depth discontinuities often manifest as strong edges in images. Conversely, audio and visual data for speech recognition have correlations at a “mid-level”, as phonemes and visemes (lip pose and motions); it can be difficult to relate raw pixels to audio waveforms or spectrograms.

In this paper, we are interested in modeling “mid-level” relationships, thus we choose to use audio-visual speech classification to validate our methods. In particular, we focus on learning representations for speech audio which are coupled with videos of the lips.

We will consider the learning settings shown in Figure 1. The overall task can be divided into three phases – feature learning, supervised training, and testing. A simple linear classifier is used for supervised training and testing to examine different feature learning models with multimodal data. In particular, we consider three learning settings – multimodal fusion, cross modality learning, and shared representation learning.

In the multimodal fusion setting, data from all modalities is available at all phases; this represents the typical setting considered in most prior work in audio-visual speech recognition (Potamianos et al., 2004). In cross modality learning, data from multiple modalities is available only during feature learning; during the supervised training and testing phase, only data from a single modality is provided. For this setting, the aim is to learn better single modality representations given unlabeled data from multiple modalities. Last, we con-

---

Appearing in *Proceedings of the 28<sup>th</sup> International Conference on Machine Learning*, Bellevue, WA, USA, 2011. Copyright 2011 by the author(s)/owner(s).

sider a shared representation learning setting, which is unique in that different modalities are presented for supervised training and testing. This setting allows us to evaluate if the feature representations can capture correlations across different modalities. Specifically, studying this setting allows us to assess whether the learned representations are modality-invariant.

In the following sections, we first describe the building blocks of our model. We then present different multimodal learning models leading to a deep network that is able to perform the various multimodal learning tasks. Finally, we report experimental results and conclude.

## 2. Background

Recent work on deep learning (Hinton & Salakhutdinov, 2006; Salakhutdinov & Hinton, 2009) has examined how deep sigmoidal networks can be trained to produce useful representations for handwritten digits and text. The key idea is to use greedy layer-wise training with Restricted Boltzmann Machines (RBMs) followed by fine-tuning. We use an extension of RBMs with sparsity (Lee et al., 2007), which have been shown to learn meaningful features for digits and natural images. In the next section, we review the sparse RBM, which is used as a layer-wise building block for our models.

### 2.1. Sparse restricted Boltzmann machines

The RBM is an undirected graphical model with hidden variables ( $\mathbf{h}$ ) and visible variables ( $\mathbf{v}$ ) (Figure 2a). There are symmetric connections between the hidden and visible variables ( $W_{i,j}$ ), but no connections within hidden variables or visible variables. The model defines a probability distribution over  $\mathbf{h}, \mathbf{v}$  (Equation 1). This particular configuration makes it easy to compute the conditional probability distributions, when  $\mathbf{v}$  or  $\mathbf{h}$  is fixed (Equation 2).

$$-\log P(\mathbf{v}, \mathbf{h}) \propto E(\mathbf{v}, \mathbf{h}) = \frac{1}{2\sigma^2} \mathbf{v}^T \mathbf{v} - \frac{1}{\sigma^2} \left( \mathbf{c}^T \mathbf{v} + \mathbf{b}^T \mathbf{h} + \mathbf{h}^T W \mathbf{v} \right) \quad (1)$$

$$p(h_j | \mathbf{v}) = \text{sigmoid}\left(\frac{1}{\sigma^2} (b_j + \mathbf{w}_j^T \mathbf{v})\right) \quad (2)$$

This formulation models the visible variables as real-valued units and the hidden variables as binary units.<sup>1</sup> As it is intractable to compute the gradient of the log-likelihood term, we learn the parameters of the

<sup>1</sup>We use Gaussian visible units for the RBM that is connected to the input data. When training the deeper layers, we use binary visible units.

|                                | Feature Learning | Supervised Training | Testing |
|--------------------------------|------------------|---------------------|---------|
| Classic Deep Learning          | Audio            | Audio               | Audio   |
|                                | Video            | Video               | Video   |
| Multimodal Fusion              | A + V            | A + V               | A + V   |
| Cross Modality Learning        | A + V            | Video               | Video   |
|                                | A + V            | Audio               | Audio   |
| Shared Representation Learning | A + V            | Audio               | Video   |
|                                | A + V            | Video               | Audio   |

Figure 1: Multimodal Learning settings where A+V refers to Audio and Video.

model ( $w_{i,j}, b_j, c_i$ ) using contrastive divergence (Hinton, 2002).

To regularize the model for sparsity (Lee et al., 2007), we encourage each hidden unit to have a pre-determined expected activation using a regularization penalty of the form  $\lambda \sum_j (\rho - \frac{1}{m} (\sum_{k=1}^m \mathbf{E}[h_j | \mathbf{v}^k]))^2$ , where  $\{\mathbf{v}^1, \dots, \mathbf{v}^m\}$  is the training set and  $\rho$  determines the sparsity of the hidden unit activations.

## 3. Learning architectures

In this section, we describe our models for the task of audio-visual bimodal feature learning, where the audio and visual input to the model are contiguous audio (spectrogram) and video frames. To motivate our deep autoencoder (Hinton & Salakhutdinov, 2006) model, we first describe several simple models and their drawbacks.

One of the most straightforward approaches to feature learning is to train a RBM model *separately* for audio and video (Figure 2a,b). After learning the RBM, the posteriors of the hidden variables given the visible variables (Equation 2) can then be used as a new representation for the data. We use this model as a baseline to compare the results of our multimodal models, as well as for pre-training the deep networks.

To train a multimodal model, a direct approach is to train a RBM over the concatenated audio and video data (Figure 2c). While this approach jointly models the distribution of the audio and video data, it is limited as a shallow model. In particular, since the correlations between the audio and video data are highly non-linear, it is hard for a RBM to learn these correlations and form multimodal representations. In practice, we found that learning a shallow bimodal RBM results in hidden units that have strong connections to variables from individual modality but few units that connect across the modalities.

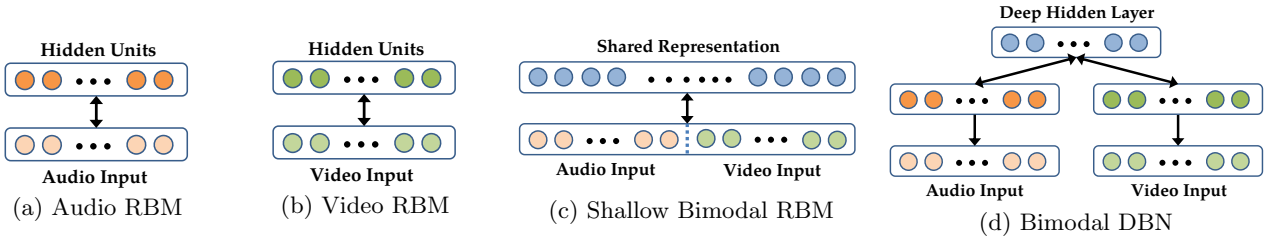


Figure 2: RBM Pretraining Models. We train RBMs for (a) audio and (b) video separately as a baseline. The shallow model (c) is limited and we find that this model is unable to capture correlations across the modalities. The bimodal deep belief network (DBN) model (d) is trained in a greedy layer-wise fashion by first training models (a) & (b). We later “unroll” the deep model (d) to train the deep autoencoder models presented in Figure 3.

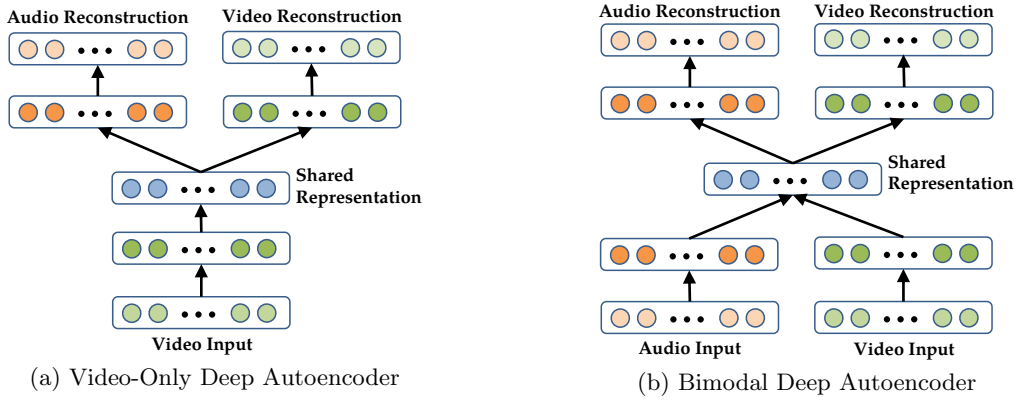


Figure 3: Deep Autoencoder Models. A “video-only” model is shown in (a) where the model learns to reconstruct both modalities given only video as the input. A similar model can be drawn for the “audio-only” setting. We train the (b) bimodal deep autoencoder in a denoising fashion, using an augmented dataset with examples that require the network to reconstruct both modalities given only one. Both models are pre-trained using sparse RBMs (Figure 2d). Since we use a sigmoid transfer function in the deep network, we can initialize the network using the conditional probability distributions  $p(\mathbf{h}|\mathbf{v})$  and  $p(\mathbf{v}|\mathbf{h})$  of the learned RBM.

Therefore, we consider greedily training a RBM over the pre-trained layers for each modality, as motivated by deep learning methods (Figure 2d).<sup>2</sup> In particular, the posteriors (Equation 2) of the first layer hidden variables are used as the training data for the new layer. By representing the data through learned first layer representations, it can be easier for the model to learn higher-order correlations across modalities. Informally, the first layer representations correspond to phonemes and visemes and the second layer models the relationships between them. Figure 4 shows visualizations of learned features from our models including examples of visual bases corresponding to visemes.

However, there are still two issues with the above multimodal models. First, there is no explicit objective for the models to discover correlations across the modalities.

<sup>2</sup>It is possible to instead learn a large RBM as the first layer that connects to both modalities. However, since a single layer RBM tends to learn unimodal units, it is much more efficient to learn separate models for each modality.

ties; it is possible for the model to find representations such that some hidden units are tuned only for audio while others are tuned only for video. Second, the models are clumsy to use in a cross modality learning setting where only one modality is present during supervised training and testing. With only a single modality present, one would need to integrate out the unobserved visible variables to perform inference.

Thus, we propose a deep autoencoder that resolves both issues. We first consider the cross modality learning setting where both modalities are present during feature learning but only a single modality is used for supervised training and testing. The deep autoencoder (Figure 3a) is trained to reconstruct both modalities when given only video data and thus discovers correlations across the modalities. Analogous to Hinton & Salakhutdinov (2006), we initialize the deep autoencoder with the bimodal DBN weights (Figure 2d) based on Equation 2, discarding any weights that are no longer present. The middle layer can be used as the

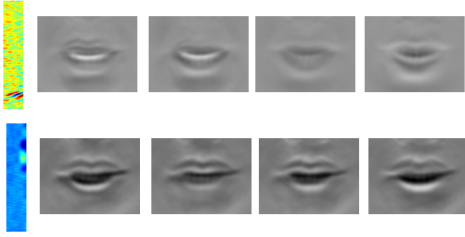


Figure 4: Visualization of learned representations. These figures correspond to two deep hidden units, where we visualize the most strongly connected first layer features. The units are presented in audio-visual pairs (we have found it generally difficult to interpret the connection between the pair). The visual bases captured lip motions and articulations, including different mouth articulations, opening and closing of the mouth, exposing teeth.

new feature representation. This model can be viewed as an instance of multitask learning (Caruana, 1997).

We use the deep autoencoder (Figure 3a) models in settings where only a single modality is present at supervised training and testing. On the other hand, when multiple modalities are available for the task (e.g., multimodal fusion), it is less clear how to use the model as one would need to train a deep autoencoder for each modality. One straightforward solution is to train the networks such that the decoding weights are tied. However, such an approach does not scale well – if we were to allow any combination of modalities to be present or absent at test time, we will need to train an exponential number of models.

Inspired by denoising autoencoders (Vincent et al., 2008), we propose training the bimodal deep autoencoder (Figure 3b) using an augmented but noisy dataset with additional examples that have only a single-modality as input. In practice, we add examples that have zero values for one of the input modalities (e.g., video) and original values for the other input modality (e.g., audio), but still require the network to reconstruct both modalities (audio and video). Thus, one-third of the training data has only video for input, while another one-third of the data has only audio, and the last one-third of the data has both audio and video.

Due to initialization using sparse RBMs, we find that the hidden units have low expected activation, even *after* the deep autoencoder training. Therefore, when one of the input modalities is set to zero, the first layer representations are also close to zero. In this case, we are essentially training a modality-specific deep autoencoder network (Figure 3a). Effectively, the method learns a model which is robust to inputs where a modality is absent.

## 4. Experiments and Results

We evaluate our methods on audio-visual speech classification of isolated letters and digits. The sparseness parameter  $\rho$  was chosen using cross-validation, while all other parameters (including hidden layer size and weight regularization) were kept fixed.<sup>3</sup>

### 4.1. Data Preprocessing

We represent the audio signal using its spectrogram<sup>4</sup> with temporal derivatives, resulting in a 483 dimension vector which was reduced to 100 dimensions with PCA whitening. 10 contiguous audio frames were used as the input to our models.

For the video, we preprocessed the frames so as to extract only the region-of-interest (ROI) encompassing the mouth.<sup>5</sup> Each mouth ROI was rescaled to  $60 \times 80$  pixels and further reduced to 32 dimensions,<sup>6</sup> using PCA whitening. Temporal derivatives over the reduced vector were also used. We used 4 contiguous video frames for input since this had approximately the same duration as 10 audio frames.

For both modalities, we also performed feature mean normalization over time (Potamianos et al., 2004), akin to removing the DC component from each example. We also note that adding temporal derivatives to the representations has been widely used in the literature as it helps to model dynamic speech information (Potamianos et al., 2004; Zhao & Barnard, 2009). The temporal derivatives were computed using a normalized linear slope so that the dynamic range of the derivative features is comparable to the original signal.

### 4.2. Datasets and Task

Since only unlabeled data was required for unsupervised feature learning, we combined diverse datasets (as listed below) to learn features. AVLetters and CUAVE were further used for supervised classification. We ensured that no test data was used for unsupervised feature learning. All deep autoencoder models were trained with all available unlabeled audio and video data.

<sup>3</sup>We cross-validated  $\rho$  over  $\{0.01, 0.03, 0.05, 0.07\}$ . The first layer features were 4x overcomplete for video (1536 units) and 1.5x overcomplete for audio (1500 units). The second layer was 1.5x the size of the combined first layers (4554 units).

<sup>4</sup>Each spectrogram frame (161 frequency bins) had a 20ms window with 10ms overlaps.

<sup>5</sup>We used an off-the-shelf object detector (Dalal & Triggs, 2005) with median filtering over time to extract the mouth regions.

<sup>6</sup>Similar to (Duchnowski et al., 1994) we found that 32 dimensions were sufficient and performed well.



**CUAVE** (Patterson et al., 2002). 36 speakers saying the digits 0 to 9. We used the *normal* portion of the dataset which contained frontal facing speakers saying each digit 5 times. We evaluated digit classification on the CUAVE dataset in a speaker independent setting. As there has not been a fixed protocol for evaluation on this dataset, we chose to use odd-numbered speakers for the test set and even-numbered speakers for the training set.

**AVLetters** (Matthews et al., 2002). 10 speakers saying the letters A to Z, three times each. The dataset provided pre-extracted lip regions of  $60 \times 80$  pixels. As the raw audio was not available for this dataset, we used it for evaluation on a visual-only lipreading task (Section 4.3). We report results on the *third-test* settings used by Zhao & Barnard (2009) and Matthews et al. (2002) for comparisons.

**AVLetters2** (Cox et al., 2008). 5 speakers saying the letters A to Z, seven times each. This is a new high-definition version of the AVLetters dataset. We used this dataset for unsupervised training only.

**Stanford Dataset**. 23 volunteers spoke the digits 0 to 9, letters A to Z and selected sentences from the TIMIT dataset. We collected this data in a similar fashion to the CUAVE dataset and used it for unsupervised training only.

**TIMIT** (Fisher et al., 1986). We used this dataset for unsupervised audio feature pre-training.

We note that in all datasets there is variability in the lips in terms of appearance, orientation and size. For each audio-video clip, features were extracted from overlapping sequences of frames. Since examples had varying durations, we divided each example into  $S$  equal slices and performed average-pooling over each slice. The features from all slices were subsequently concatenated together. Specifically, we combined features using  $S = 1$  and  $S = 3$  to form our final feature representation for classification with a linear SVM.

### 4.3. Cross Modality Learning

In the cross modality learning experiments, we evaluate if we can learn better representations for one modality (e.g., video) when given multiple modalities (e.g., audio and video) during feature learning.

On the AVLetters dataset (Table 1a), our deep autoencoder models show a significant improvement over hand-engineered features from prior work. The video-only deep autoencoder performed the best on the dataset, obtaining a classification accuracy of 64.4%, outperforming the best previous published results.

On the CUAVE dataset (Table 1b), there is an improvement by learning video features with both video

and audio compared to learning features with only video data (although not performing as well as state-of-the-art). In our models, we chose to use a very simple front-end that only extracts bounding boxes, without any correction for orientation or perspective changes. In contrast, recent AAM models (Papandreou et al., 2009) are trained to accurately track the speaker’s face and further register the face with a mean face template, canceling shape deformations. Combining these sophisticated visual front-ends with our features has the potential to do even better.

Table 1: Classification performance for visual speech classification on (a) AVLetters and (b) CUAVE. Deep autoencoders perform the best and show effective cross modality learning. Where indicated, the error bars show the variation ( $\pm 2$  s.d.) due to random initialization. §Results are on continuous speech recognition performance, though we note that the *normal* portion of CUAVE has speakers saying isolated digits. †These models use a visual front-end system that is significantly more complicated than ours and a different train/test split.

| Feature Representation                                 | Accuracy                         |
|--|----------------------------------|
| Baseline Preprocessed Video                            | 46.2%                            |
| RBM Video (Figure 2b)                                  | 54.2% $\pm$ 3.3%                 |
| <b>Video-Only Deep Autoencoder</b><br>(Figure 3a)      | <b>64.4%<math>\pm</math>2.4%</b> |
| Bimodal Deep Autoencoder<br>(Figure 3b)                | 59.2%                            |
| Multiscale Spatial Analysis<br>(Matthews et al., 2002) | 44.6%                            |
| Local Binary Pattern<br>(Zhao & Barnard, 2009)         | 58.85%                           |

(a) AVLetters

| Feature Representation                               | Accuracy                         |
|--|----------------------------------|
| Baseline Preprocessed Video                          | 58.5%                            |
| RBM Video (Figure 2b)                                | 65.4% $\pm$ 0.6%                 |
| <b>Video-Only Deep Autoencoder</b><br>(Figure 3a)    | <b>68.7%<math>\pm</math>1.8%</b> |
| Bimodal Deep Autoencoder<br>(Figure 3b)              | 66.7%                            |
| Discrete Cosine Transform<br>(Gurban & Thiran, 2009) | 64% †§                           |
| Active Appearance Model<br>(Papandreou et al., 2007) | 75.7% †                          |
| Active Appearance Model<br>(Pitsikalis et al., 2006) | 68.7% †                          |
| Fused Holistic+Patch<br>(Lucey & Sridharan, 2006)    | 77.08% †                         |
| Visemic AAM<br>(Papandreou et al., 2009)             | 83% †§                           |

(b) CUAVE Video

Table 2: Digit classification performance for bimodal speech classification on CUAVE, under clean and noisy conditions. We added white Gaussian noise to the original audio signal at 0 dB SNR. The error bars reflect the variation ( $\pm 2$  s.d.) of the results due to the random noise added to the audio data. We compare performance of the Bimodal Deep Autoencoder model with the best audio features (Audio RBM) and the best video features (Video-only Deep Autoencoder).

| Feature Representation                      | Accuracy<br>(Clean Audio) | Accuracy<br>(Noisy Audio) |
|---|---------------------------|---------------------------|
| (a) Audio RBM (Figure 2a)                   | <b>95.8%</b>              | 75.8% $\pm$ 2.0%          |
| (b) Video-only Deep Autoencoder (Figure 3a) | 68.7%                     | 68.7%                     |
| (c) Bimodal Deep Autoencoder (Figure 3b)    | 90.0%                     | 77.3% $\pm$ 1.4%          |
| (d) <b>Bimodal + Audio RBM</b>              | 94.4%                     | <b>82.2%</b> $\pm$ 1.2%   |
| (e) Video-only Deep AE + Audio-RBM          | 87.0%                     | 76.6% $\pm$ 0.8%          |

These video classification results show that the deep autoencoders achieve cross modality learning by discovering better video representations when given additional audio data. In particular, even though the AVLetters dataset did not have any audio data, we were able to improve performance by learning better video features using other additional unlabeled audio and video data.

However, the bimodal deep autoencoder did not perform as well as the video-only deep autoencoder: while the video-only autoencoder learns only video features (which are also good for audio reconstruction), the bimodal autoencoder learns audio-only, video-only and invariant features. As such, the feature set learned by the bimodal autoencoder might not be optimal when the task at hand has only visual input.

We also note that cross modality learning for audio did not improve classification results compared to using audio RBM features; audio features are highly discriminative for speech classification, adding video information can sometimes hurt performance.

#### 4.4. Multimodal Fusion Results

While using audio information alone performs reasonably well for speech recognition, fusing audio and video information can substantially improve performance, especially when the audio is degraded with noise (Gurban & Thiran, 2009; Papandreou et al., 2007; Pitsikalis et al., 2006; Papandreou et al., 2009). In particular, it is common to find that audio features perform well on their own and concatenating video features can sometimes hurt performance. Hence, we evaluate our models in both clean and noisy audio settings.

The video modality complements the audio modality by providing information such as place of articulation, which can help distinguish between similar sounding speech. However, when one simply concatenates audio and visual features (Table 2e), it is often the case that performance is worse as compared to using only audio features (Table 2a). Since our models are able to learn

multimodal features that go beyond simply concatenating the audio and visual features, we propose combining the audio features with our multimodal features (Table 2d). When the best audio features are concatenated with the bimodal features, it outperforms the other feature combinations. This shows that the learned multimodal features are better able to complement the audio features.

#### 4.5. McGurk effect

Table 3: McGurk Effect

| Audio / Visual<br>Setting | Model prediction |       |       |
|---------------------------|------------------|-------|-------|
|                           | /ga/             | /ba/  | /da/  |
| Visual /ga/, Audio /ga/   | 82.6%            | 2.2%  | 15.2% |
| Visual /ba/, Audio /ba/   | 4.4%             | 89.1% | 6.5%  |
| Visual /ga/, Audio /ba/   | 28.3%            | 13.0% | 58.7% |

The McGurk effect (McGurk & MacDonald, 1976) refers to an audio-visual perception phenomenon where a visual /ga/ with a audio /ba/ is perceived as /da/ by most subjects. Since our model learns a multimodal representation, it would be interesting to observe if the model is able to replicate a similar effect.

We obtained data from 23 volunteers speaking 5 repetitions of /ga/, /ba/ and /da/. The bimodal deep autoencoder features<sup>7</sup> were used to train a linear SVM on this 3-way classification task. The model was tested on three conditions that simulate the McGurk effect. When the visual and audio data matched at test time, the model was able to predict the correct class /ba/ and /ga/ with an accuracy of 82.6% and 89.1% respectively. On the other hand, when a visual /ga/ with a voiced /ba/ was mixed at test time, the model was most likely to predict /da/, even though /da/ neither appears in the visual nor audio inputs, consistent with the McGurk effect on people. The same effect was not observed with the bimodal DBN (Figure 2d) or with concatenating audio and video RBM features.

<sup>7</sup>The /ga/, /ba/ and /da/ data was not used for training the bimodal deep autoencoder.

#### 4.6. Shared Representation Learning

Table 4: Shared representation learning on CUAVE. Chance performance is at 10%.

| Train/Test  | Method                  | Accuracy     |
|-------------|-------------------------|--------------|
| Audio/Video | Raw-CCA                 | 41.9%        |
|             | <b>RBM-CCA Features</b> | <b>57.3%</b> |
|             | Bimodal Deep AE         | 30.7%        |
| Video/Audio | Raw-CCA                 | 42.9%        |
|             | <b>RBM-CCA Features</b> | <b>91.7%</b> |
|             | Bimodal Deep AE         | 24.3%        |

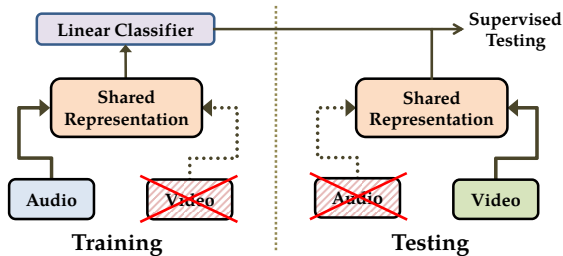


Figure 5: “Hearing to see” setting (train on audio, test on video) for evaluating shared representations.

In this experiment, we propose a novel setting which examines if a shared representation can be learned over audio and video speech data. During supervised training, the algorithm is provided data solely from one modality (e.g., audio) and later tested only on the other modality (e.g., video), as shown in Figure 5. In essence, we are telling the supervised learner how the digits “1”, “2”, etc. *sound*, while asking it to distinguish them based on how they are visually spoken – “hearing to see”. If we are able to capture the correlations across the modalities in our shared representation, the model will perform this task well.

One approach to learning a shared representation is to find transformations for the modalities that maximize correlations. In particular, we suggest using canonical correlation analysis (CCA) (Hardoon et al., 2004), which finds linear transformations of audio and video data, to form a shared representation.<sup>8</sup> Learning a CCA shared representation on raw data results in surprisingly good performance (Table 4: Raw-CCA). However, learning the CCA representation on the first layer features (i.e., Audio RBM and Video RBM features) results in significantly better performance, comparable to using the original modalities for supervised classification (Table 4: RBM-CCA Features). This is particularly surprising since testing on audio performs

<sup>8</sup>Given audio data  $\mathbf{a}$  and video data  $\mathbf{v}$ , CCA finds matrices  $P$  and  $Q$  such that  $P\mathbf{a}$  and  $Q\mathbf{v}$  have maximum correlations.

better than testing on video, even when the model was trained on video data. These results show that capturing relationships across the modalities require at least a single non-linear stage to be successful. When good features have been learned from both modalities, a linear model can be well suited to capture the relationships. However, it is important to note that CCA, a linear transformation, does not help in other tasks such as cross-modality learning.

We further used this task to examine whether the features from the bimodal deep autoencoder captures correlations across the modalities.<sup>9</sup> While the bimodal deep autoencoder model does not perform as well as CCA, the results show that our learned representations are partially invariant to the input modality.

#### 4.7. Additional Control Experiments

The video-only deep autoencoder has audio as a training cue and multiple hidden layers (Figure 3a). We first considered removing audio as a cue by training a similar deep autoencoder that did not reconstruct audio data; the performance decreased by 7.7% on CUAVE and 14.3% on AVLetters. Next, we trained a video-only shallow autoencoder with a single hidden layer to reconstruct both audio and video<sup>10</sup>; the performance decreased by 2.1% on CUAVE and 5.0% on AVLetters. Hence, both audio as a cue and depth were important ingredients for the video-only deep autoencoder to perform well.

We also compared the performance of using the bimodal DBN without training it as an autoencoder. In cases where only one modality was present, we used the same approach as the bimodal deep autoencoder, setting the absent modality to zero.<sup>11</sup> The bimodal DBN performed worse in the cross-modality and shared representation tasks and did not show the McGurk effect. It performed comparably on the multimodal fusion task.<sup>12</sup>

<sup>9</sup>For the bimodal deep autoencoder, we set the value of the absent modality to zero when computing the shared representation, which is consistent with the feature learning phase.

<sup>10</sup>The single hidden layer takes video as input and reconstructs both audio and video.

<sup>11</sup>We also tried alternating Gibbs sampling to obtain the posterior, but the results were worse.

<sup>12</sup>For the video-only setting, the bimodal DBN performed 4.9% worse on the CUAVE dataset and 5.0% worse on the AVLetters dataset. It was at chance on the “hearing to see” task and obtained 28.1% on “seeing to hear”.

## 5. Related Work

While we present special cases of neural networks for multimodal learning, we note that prior work on audio-visual speech recognition (Duchnowski et al., 1994; Yuhás et al., 1989; Meier et al., 1996; Bregler & Konig, 1994) has also explored the use of neural networks. Yuhás et al. (1989) trained a neural network to predict the auditory signal given the visual input. They showed improved performance in a noisy setting when they combined the predicted auditory signal (from the network using visual input) with a noisy auditory signal. Duchnowski et al. (1994) and Meier et al. (1996) trained separate networks to model phonemes and visemes and combined the predictions at a phonetic layer to predict the spoken phoneme.

In contrast to these approaches, we use the hidden units to build a new representation of the data. Furthermore, we do not model phonemes or visemes, which require expensive labeling efforts. Finally, we build deep bimodal representations by modeling the correlations across the learned shallow representations.

## 6. Discussion

Hand-engineering task-specific features is often difficult and time consuming. For example, it is not immediately clear what the appropriate features should be for lipreading (visual-only data). This difficulty is more pronounced with multimodal data as the features have to relate multiple data sources. In this work, we showed how deep learning can be applied to this challenging task for discovering multimodal features.

## Acknowledgments

We thank Clemson University for providing the CUAVE dataset and University of Surrey for providing the AVLetters2 dataset. We also thank Quoc Le, Andrew Saxe, Andrew Maas, and Adam Coates for insightful discussions, and the anonymous reviewers for helpful comments. This work is supported by the DARPA Deep Learning program under contract number FA8650-10-C-7020.

## References

- Bregler, C. and Konig, Y. "Eigenlips" for robust speech recognition. In *ICASSP*, 1994.
- Caruana, R. Multitask learning. *Machine Learning*, 28(1): 41–75, 1997.
- Cox, S., Harvey, R., Lan, Y., and Newman, J. The challenge of multispeaker lip-reading. In *International Conference on Auditory-Visual Speech Processing*, 2008.
- Dalal, N. and Triggs, B. Histograms of Oriented Gradients for Human Detection. In *CVPR*, 2005.
- Duchnowski, P., Meier, U., and Waibel, A. See me, hear me: Integrating automatic speech recognition and lipreading. In *ICSLP*, pp. 547–550, 1994.
- Fisher, W., Doddington, G., and Marshall, Goudie. The DARPA speech recognition research database: Specification and status. In *DARPA Speech Recognition Workshop*, pp. 249–249, 1986.
- Gurban, M. and Thiran, J.P. Information theoretic feature extraction for audio-visual speech recognition. *IEEE Trans. on Sig. Proc.*, 57(12):4765–4776, 2009.
- Hardoon, David R., Szedmak, Sandor R., and Shawe-taylor, John R. Canonical correlation analysis: An overview with application to learning methods. *Neural Computation*, 16:2639–2664, 2004.
- Hinton, G. Training products of experts by minimizing contrastive divergence. *Neural Computation*, 2002.
- Hinton, G. and Salakhutdinov, R. Reducing the dimensionality of data with neural networks. *Science*, 313(5786): 504–507, 2006.
- Lee, H., Ekanadham, C., and Ng, A. Sparse deep belief net model for visual area V2. In *NIPS*, 2007.
- Lucey, P. and Sridharan, S. Patch-based representation of visual speech. In *HCSNet Workshop on the Use of Vision in Human-Computer Interaction*, 2006.
- Matthews, I., Cootes, T.F., Bangham, J.A., and Cox, S. Extraction of visual features for lipreading. *PAMI*, 24: 198–213, 2002.
- McGurk, H. and MacDonald, J. Hearing lips and seeing voices. *Nature*, 264(5588):746–748, 1976.
- Meier, U., Hürst, W., and Duchnowski, P. Adaptive Bimodal Sensor Fusion For Automatic Speechreading. In *ICASSP*, pp. 833–836, 1996.
- Papandreou, G., Katsamanis, A., Pitsikalis, V., and Maragos, P. Multimodal fusion and learning with uncertain features applied to audiovisual speech recognition. In *MMSP*, pp. 264–267, 2007.
- Papandreou, G., Katsamanis, A., Pitsikalis, V., and Maragos, P. Adaptive multimodal fusion by uncertainty compensation with application to audiovisual speech recognition. *IEEE TASLP*, 17(3):423–435, 2009.
- Patterson, E., Gurbuz, S., Tufekci, Z., and Gowdy, J. CUAVE: A new audio-visual database for multimodal human-computer interface research. 2:2017–2020, 2002.
- Pitsikalis, V., Katsamanis, A., Papandreou, G., and Maragos, P. Adaptive multimodal fusion by uncertainty compensation. In *ICSLP*, pp. 2458–2461, 2006.
- Potamianos, G., Neti, C., Luetttin, J., and Matthews, I. Audio-visual automatic speech recognition: An overview. In *Issues in Visual and Audio-Visual Speech Processing*. MIT Press, 2004.
- Salakhutdinov, R. and Hinton, G. Semantic hashing. *IJAR*, 50(7):969–978, 2009.
- Summerfield, Q. Lipreading and audio-visual speech perception. *Trans. R. Soc. Lond.*, pp. 71–78, 1992.
- Vincent, P., Larochelle, H., Bengio, Y., and Manzagol, P.A. Extracting and composing robust features with denoising autoencoders. In *ICML*, pp. 1096–1103. ACM, 2008.
- Yuhás, B. P., Goldstein, M. H., and Sejnowski, T. J. Integration of acoustic and visual speech signals using neural networks. *IEEE Comm. Magazine*, pp. 65–71, 1989.
- Zhao, G. and Barnard, M. Lipreading with local spatiotemporal descriptors. *IEEE Transactions on Multimedia*, 11(7):1254–1265, 2009.



## PDF Form Example

This is an example of a user fillable PDF form. Normally PDF is used as a final publishing format. However PDF has an option to be used as an entry form that can be edited and saved by the user.

The fields of this form have been selected to demonstrate as many as possible of the common entry fields.

This document and PDF form have been created with OpenOffice (version 3.4.0).

To fill out the form, make sure the PDF file is not read-only. If the file is read-only save it first to a folder or computer desktop. Close this file and open the saved file.

Please fill out the following fields. Important fields are marked yellow.

Given Name:

second annotation test

Family Name:

Address 1:

House nr:

Address 2:

Postcode:

City:

Country:

Gender:

Height (cm):

Driving License:

I speak at least 3 languages

☐ Deutsch

☐ English

☐ Esperanto

☐ Latin

Favourite colour:

**Important:** Save the completed PDF form (use menu File - Save).

# Trace-based Just-in-Time Type Specialization for Dynamic Languages

Andreas Gal<sup>\*,+</sup>, Brendan Eich<sup>\*</sup>, Mike Shaver<sup>\*</sup>, David Anderson<sup>\*</sup>, David Mandelin<sup>\*</sup>,  
Mohammad R. Haghighat<sup>§</sup>, Blake Kaplan<sup>\*</sup>, Graydon Hoare<sup>\*</sup>, Boris Zbarsky<sup>\*</sup>, Jason Orendorff<sup>\*</sup>,  
Jesse Ruderman<sup>\*</sup>, Edwin Smith<sup>#</sup>, Rick Reitmaier<sup>#</sup>, Michael Bebenita<sup>+</sup>, Mason Chang<sup>+,#</sup>, Michael Franz<sup>+</sup>

Mozilla Corporation<sup>\*</sup>

{gal,brendan,shaver,danderson,dmandelin,mrbkap,graydon,bz,jorendorff,jruderman}@mozilla.com

Adobe Corporation<sup>#</sup>

{edwsmith,rreitmai}@adobe.com

Intel Corporation<sup>§</sup>

{mohammad.r.haghighat}@intel.com

University of California, Irvine<sup>+</sup>

{mbebenit,changm,franz}@uci.edu

## Abstract

Dynamic languages such as JavaScript are more difficult to compile than statically typed ones. Since no concrete type information is available, traditional compilers need to emit generic code that can handle all possible type combinations at runtime. We present an alternative compilation technique for dynamically-typed languages that identifies frequently executed loop traces at run-time and then generates machine code on the fly that is specialized for the actual dynamic types occurring on each path through the loop. Our method provides cheap inter-procedural type specialization, and an elegant and efficient way of incrementally compiling lazily discovered alternative paths through nested loops. We have implemented a dynamic compiler for JavaScript based on our technique and we have measured speedups of 10x and more for certain benchmark programs.

**Categories and Subject Descriptors** D.3.4 [Programming Languages]: Processors — Incremental compilers, code generation.

**General Terms** Design, Experimentation, Measurement, Performance.

**Keywords** JavaScript, just-in-time compilation, trace trees.

## 1. Introduction

*Dynamic languages* such as JavaScript, Python, and Ruby, are popular since they are expressive, accessible to non-experts, and make deployment as easy as distributing a source file. They are used for small scripts as well as for complex applications. JavaScript, for example, is the de facto standard for client-side web programming

and is used for the application logic of browser-based productivity applications such as Google Mail, Google Docs and Zimbra Collaboration Suite. In this domain, in order to provide a fluid user experience and enable a new generation of applications, virtual machines must provide a low startup time and high performance.

Compilers for statically typed languages rely on type information to generate efficient machine code. In a dynamically typed programming language such as JavaScript, the types of expressions may vary at runtime. This means that the compiler can no longer easily transform operations into machine instructions that operate on one specific type. Without exact type information, the compiler must emit slower generalized machine code that can deal with all potential type combinations. While compile-time static type inference might be able to gather type information to generate optimized machine code, traditional static analysis is very expensive and hence not well suited for the highly interactive environment of a web browser.

We present a trace-based compilation technique for dynamic languages that reconciles speed of compilation with excellent performance of the generated machine code. Our system uses a mixed-mode execution approach: the system starts running JavaScript in a fast-starting bytecode interpreter. As the program runs, the system identifies *hot* (frequently executed) bytecode sequences, records them, and compiles them to fast native code. We call such a sequence of instructions a *trace*.

Unlike method-based dynamic compilers, our dynamic compiler operates at the granularity of individual loops. This design choice is based on the expectation that programs spend most of their time in hot loops. Even in dynamically typed languages, we expect hot loops to be mostly *type-stable*, meaning that the types of values are invariant. (12) For example, we would expect loop counters that start as integers to remain integers for all iterations. When both of these expectations hold, a trace-based compiler can cover the program execution with a small number of type-specialized, efficiently compiled traces.

Each compiled trace covers one path through the program with one mapping of values to types. When the VM executes a compiled trace, it cannot guarantee that the same path will be followed or that the same types will occur in subsequent loop iterations.

Permission to make digital or hard copies of all or part of this work for personal or classroom use is granted without fee provided that copies are not made or distributed for profit or commercial advantage and that copies bear this notice and the full citation on the first page. To copy otherwise, to republish, to post on servers or to redistribute to lists, requires prior specific permission and/or a fee.

PLDI'09, June 15–20, 2009, Dublin, Ireland.

Copyright © 2009 ACM 978-1-60558-392-1/09/06...\$5.00

Hence, recording and compiling a trace *speculates* that the path and typing will be exactly as they were during recording for subsequent iterations of the loop.

Every compiled trace contains all the *guards* (checks) required to validate the speculation. If one of the guards fails (if control flow is different, or a value of a different type is generated), the trace exits. If an exit becomes hot, the VM can record a *branch trace* starting at the exit to cover the new path. In this way, the VM records a *trace tree* covering all the hot paths through the loop.

Nested loops can be difficult to optimize for tracing VMs. In a naïve implementation, inner loops would become hot first, and the VM would start tracing there. When the inner loop exits, the VM would detect that a different branch was taken. The VM would try to record a branch trace, and find that the trace reaches not the inner loop header, but the outer loop header. At this point, the VM could continue tracing until it reaches the inner loop header again, thus tracing the outer loop inside a trace tree for the inner loop. But this requires tracing a copy of the outer loop for every side exit and type combination in the inner loop. In essence, this is a form of unintended tail duplication, which can easily overflow the code cache. Alternatively, the VM could simply stop tracing, and give up on ever tracing outer loops.

We solve the nested loop problem by recording *nested trace trees*. Our system traces the inner loop exactly as the naïve version. The system stops extending the inner tree when it reaches an outer loop, but then it starts a new trace at the outer loop header. When the outer loop reaches the inner loop header, the system tries to call the trace tree for the inner loop. If the call succeeds, the VM records the call to the inner tree as part of the outer trace and finishes the outer trace as normal. In this way, our system can trace any number of loops nested to any depth without causing excessive tail duplication.

These techniques allow a VM to dynamically translate a program to nested, type-specialized trace trees. Because traces can cross function call boundaries, our techniques also achieve the effects of inlining. Because traces have no internal control-flow joins, they can be optimized in linear time by a simple compiler (10). Thus, our tracing VM efficiently performs the same kind of optimizations that would require interprocedural analysis in a static optimization setting. This makes tracing an attractive and effective tool to type specialize even complex function call-rich code.

We implemented these techniques for an existing JavaScript interpreter, SpiderMonkey. We call the resulting tracing VM *TraceMonkey*. TraceMonkey supports all the JavaScript features of SpiderMonkey, with a 2x-20x speedup for traceable programs.

This paper makes the following contributions:

- We explain an algorithm for dynamically forming trace trees to cover a program, representing nested loops as nested trace trees.
- We explain how to speculatively generate efficient type-specialized code for traces from dynamic language programs.
- We validate our tracing techniques in an implementation based on the SpiderMonkey JavaScript interpreter, achieving 2x-20x speedups on many programs.

The remainder of this paper is organized as follows. Section 3 is a general overview of trace tree based compilation we use to capture and compile frequently executed code regions. In Section 4 we describe our approach of covering nested loops using a number of individual trace trees. In Section 5 we describe our trace-compilation based speculative type specialization approach we use to generate efficient machine code from recorded bytecode traces. Our implementation of a dynamic type-specializing compiler for JavaScript is described in Section 6. Related work is discussed in Section 8. In Section 7 we evaluate our dynamic compiler based on

```

1 for (var i = 2; i < 100; ++i) {
2   if (!primes[i])
3     continue;
4   for (var k = i + i; i < 100; k += i)
5     primes[k] = false;
6 }

```

**Figure 1. Sample program: sieve of Eratosthenes.** `primes` is initialized to an array of 100 false values on entry to this code snippet.

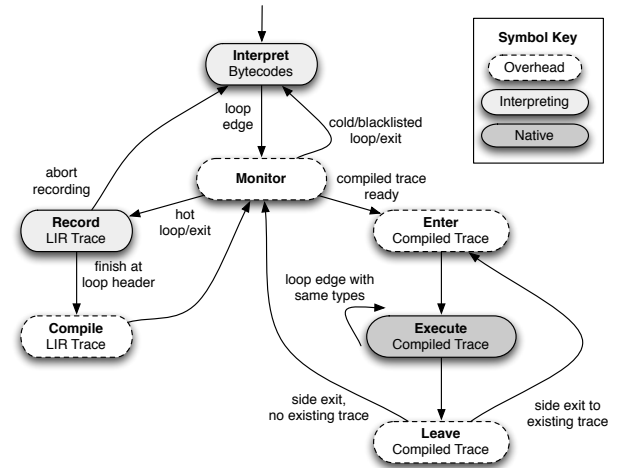


**Figure 2. State machine** describing the major activities of TraceMonkey and the conditions that cause transitions to a new activity. In the dark box, TM executes JS as compiled traces. In the light gray boxes, TM executes JS in the standard interpreter. White boxes are overhead. Thus, to maximize performance, we need to maximize time spent in the darkest box and minimize time spent in the white boxes. The best case is a loop where the types at the loop edge are the same as the types on entry—then TM can stay in native code until the loop is done.

a set of industry benchmarks. The paper ends with conclusions in Section 9 and an outlook on future work is presented in Section 10.

## 2. Overview: Example Tracing Run

This section provides an overview of our system by describing how TraceMonkey executes an example program. The example program, shown in Figure 1, computes the first 100 prime numbers with nested loops. The narrative should be read along with Figure 2, which describes the activities TraceMonkey performs and when it transitions between the loops.

TraceMonkey always begins executing a program in the bytecode interpreter. Every loop back edge is a potential trace point. When the interpreter crosses a loop edge, TraceMonkey invokes the *trace monitor*, which may decide to record or execute a native trace. At the start of execution, there are no compiled traces yet, so the trace monitor counts the number of times each loop back edge is executed until a loop becomes *hot*, currently after 2 crossings. Note that the way our loops are compiled, the loop edge is crossed before entering the loop, so the second crossing occurs immediately after the first iteration.

Here is the sequence of events broken down by outer loop iteration:

```

v0 := ld state[748]    // load primes from the trace activation record
      st sp[0], v0    // store primes to interpreter stack
v1 := ld state[764]    // load k from the trace activation record
v2 := i2f(v1)         // convert k from int to double
      st sp[8], v1    // store k to interpreter stack
      st sp[16], 0    // store false to interpreter stack
v3 := ld v0[4]        // load class word for primes
v4 := and v3, -4      // mask out object class tag for primes
v5 := eq v4, Array    // test whether primes is an array
      xf v5          // side exit if v5 is false
v6 := js_Array_set(v0, v2, false) // call function to set array element
v7 := eq v6, 0        // test return value from call
      xt v7          // side exit if js_Array_set returns false.

```

**Figure 3. LIR snippet for sample program.** This is the LIR recorded for line 5 of the sample program in Figure 1. The LIR encodes the semantics in SSA form using temporary variables. The LIR also encodes all the stores that the interpreter would do to its data stack. Sometimes these stores can be optimized away as the stack locations are live only on exits to the interpreter. Finally, the LIR records guards and side exits to verify the assumptions made in this recording: that `primes` is an array and that the call to set its element succeeds.

```

mov edx, ebx(748)    // load primes from the trace activation record
mov edi(0), edx      // (*) store primes to interpreter stack
mov esi, ebx(764)    // load k from the trace activation record
mov edi(8), esi      // (*) store k to interpreter stack
mov edi(16), 0       // (*) store false to interpreter stack
mov eax, edx(4)      // (*) load object class word for primes
and eax, -4          // (*) mask out object class tag for primes
cmp eax, Array       // (*) test whether primes is an array
jne side_exit_1      // (*) side exit if primes is not an array
sub esp, 8           // bump stack for call alignment convention
push false           // push last argument for call
push esi             // push first argument for call
call js_Array_set    // call function to set array element
add esp, 8           // clean up extra stack space
mov ecx, ebx         // (*) created by register allocator
test eax, eax        // (*) test return value of js_Array_set
je side_exit_2       // (*) side exit if call failed
...
side_exit_1:
mov ecx, ebp(-4)     // restore ecx
mov esp, ebp         // restore esp
jmp epilg           // jump to ret statement

```

**Figure 4. x86 snippet for sample program.** This is the x86 code compiled from the LIR snippet in Figure 3. Most LIR instructions compile to a single x86 instruction. Instructions marked with (\*) would be omitted by an idealized compiler that knew that none of the side exits would ever be taken. The 17 instructions generated by the compiler compare favorably with the 100+ instructions that the interpreter would execute for the same code snippet, including 4 indirect jumps.

**i=2.** This is the first iteration of the outer loop. The loop on lines 4-5 becomes hot on its second iteration, so TraceMonkey enters recording mode on line 4. In recording mode, TraceMonkey records the code along the trace in a low-level compiler intermediate representation we call *LIR*. The LIR trace encodes all the operations performed and the types of all operands. The LIR trace also encodes *guards*, which are checks that verify that the control flow and types are identical to those observed during trace recording. Thus, on later executions, if and only if all guards are passed, the trace has the required program semantics.

TraceMonkey stops recording when execution returns to the loop header or exits the loop. In this case, execution returns to the loop header on line 4.

After recording is finished, TraceMonkey compiles the trace to native code using the recorded type information for optimization. The result is a native code fragment that can be entered if the

**nte** interpreter PC and the types of values match those observed when trace recording was started. The first trace in our example,  $T_{45}$ , covers lines 4 and 5. This trace can be entered if the PC is at line 4, `i` and `k` are integers, and `primes` is an object. After compiling  $T_{45}$ , TraceMonkey returns to the interpreter and loops back to line 1.

**i=3.** Now the loop header at line 1 has become hot, so TraceMonkey starts recording. When recording reaches line 4, TraceMonkey observes that it has reached an inner loop header that already has a compiled trace, so TraceMonkey attempts to nest the inner loop inside the current trace. The first step is to call the inner trace as a subroutine. This executes the loop on line 4 to completion and then returns to the recorder. TraceMonkey verifies that the call was successful and then records the call to the inner trace as part of the current trace. Recording continues until execution reaches line 1, and at which point TraceMonkey finishes and compiles a trace for the outer loop,  $T_{16}$ .



**i=4.** On this iteration, TraceMonkey calls  $T_{16}$ . Because  $i=4$ , the `if` statement on line 2 is taken. This branch was not taken in the original trace, so this causes  $T_{16}$  to fail a guard and take a side exit. The exit is not yet hot, so TraceMonkey returns to the interpreter, which executes the `continue` statement.

**i=5.** TraceMonkey calls  $T_{16}$ , which in turn calls the nested trace  $T_{45}$ .  $T_{16}$  loops back to its own header, starting the next iteration without ever returning to the monitor.

**i=6.** On this iteration, the side exit on line 2 is taken again. This time, the side exit becomes hot, so a trace  $T_{23,1}$  is recorded that covers line 3 and returns to the loop header. Thus, the end of  $T_{23,1}$  jumps directly to the start of  $T_{16}$ . The side exit is patched so that on future iterations, it jumps directly to  $T_{23,1}$ .

At this point, TraceMonkey has compiled enough traces to cover the entire nested loop structure, so the rest of the program runs entirely as native code.

### 3. Trace Trees

In this section, we describe traces, trace trees, and how they are formed at run time. Although our techniques apply to any dynamic language interpreter, we will describe them assuming a bytecode interpreter to keep the exposition simple.

#### 3.1 Traces

A *trace* is simply a program path, which may cross function call boundaries. TraceMonkey focuses on *loop traces*, that originate at a loop edge and represent a single iteration through the associated loop.

Similar to an extended basic block, a trace is only entered at the top, but may have many exits. In contrast to an extended basic block, a trace can contain join nodes. Since a trace always only follows one single path through the original program, however, join nodes are not recognizable as such in a trace and have a single predecessor node like regular nodes.

A *typed trace* is a trace annotated with a type for every variable (including temporaries) on the trace. A typed trace also has an entry *type map* giving the required types for variables used on the trace before they are defined. For example, a trace could have a type map ( $x$ : `int`,  $b$ : `boolean`), meaning that the trace may be entered only if the value of the variable  $x$  is of type `int` and the value of  $b$  is of type `boolean`. The entry type map is much like the signature of a function.

In this paper, we only discuss typed loop traces, and we will refer to them simply as “traces”. The key property of typed loop traces is that they can be compiled to efficient machine code using the same techniques used for typed languages.

In TraceMonkey, traces are recorded in trace-flavored SSA LIR (low-level intermediate representation). In trace-flavored SSA (or TSSA), phi nodes appear only at the entry point, which is reached both on entry and via loop edges. The important LIR primitives are constant values, memory loads and stores (by address and offset), integer operators, floating-point operators, function calls, and conditional exits. Type conversions, such as integer to double, are represented by function calls. This makes the LIR used by TraceMonkey independent of the concrete type system and type conversion rules of the source language. The LIR operations are generic enough that the backend compiler is language independent. Figure 3 shows an example LIR trace.

Bytecode interpreters typically represent values in a various complex data structures (e.g., hash tables) in a boxed format (i.e., with attached type tag bits). Since a trace is intended to represent efficient code that eliminates all that complexity, our traces operate on unboxed values in simple variables and arrays as much as possible.

A trace records all its intermediate values in a small activation record area. To make variable accesses fast on trace, the trace also imports local and global variables by unboxing them and copying them to its activation record. Thus, the trace can read and write these variables with simple loads and stores from a native activation recording, independently of the boxing mechanism used by the interpreter. When the trace exits, the VM boxes the values from this native storage location and copies them back to the interpreter structures.

For every control-flow branch in the source program, the recorder generates conditional exit LIR instructions. These instructions exit from the trace if required control flow is different from what it was at trace recording, ensuring that the trace instructions are run only if they are supposed to. We call these instructions *guard* instructions.

Most of our traces represent loops and end with the special `loop` LIR instruction. This is just an unconditional branch to the top of the trace. Such traces return only via guards.

Now, we describe the key optimizations that are performed as part of recording LIR. All of these optimizations reduce complex dynamic language constructs to simple typed constructs by specializing for the current trace. Each optimization requires guard instructions to verify their assumptions about the state and exit the trace if necessary.

#### Type specialization.

All LIR primitives apply to operands of specific types. Thus, LIR traces are necessarily type-specialized, and a compiler can easily produce a translation that requires no type dispatches. A typical bytecode interpreter carries tag bits along with each value, and to perform any operation, must check the tag bits, dynamically dispatch, mask out the tag bits to recover the untagged value, perform the operation, and then reapply tags. LIR omits everything except the operation itself.

A potential problem is that some operations can produce values of unpredictable types. For example, reading a property from an object could yield a value of any type, not necessarily the type observed during recording. The recorder emits guard instructions that conditionally exit if the operation yields a value of a different type from that seen during recording. These guard instructions guarantee that as long as execution is on trace, the types of values match those of the typed trace. When the VM observes a side exit along such a type guard, a new typed trace is recorded originating at the side exit location, capturing the new type of the operation in question.

**Representation specialization: objects.** In JavaScript, name lookup semantics are complex and potentially expensive because they include features like object inheritance and `eval`. To evaluate an object property read expression like `o.x`, the interpreter must search the property map of `o` and all of its prototypes and parents. Property maps can be implemented with different data structures (e.g., per-object hash tables or shared hash tables), so the search process also must dispatch on the representation of each object found during search. TraceMonkey can simply observe the result of the search process and record the simplest possible LIR to access the property value. For example, the search might find the value of `o.x` in the prototype of `o`, which uses a shared hash-table representation that places `x` in slot 2 of a property vector. Then the recorded can generate LIR that reads `o.x` with just two or three loads: one to get the prototype, possibly one to get the property value vector, and one more to get slot 2 from the vector. This is a vast simplification and speedup compared to the original interpreter code. Inheritance relationships and object representations can change during execution, so the simplified code requires guard instructions that ensure the object representation is the same. In TraceMonkey, objects’ rep-

representations are assigned an integer key called the *object shape*. Thus, the guard is a simple equality check on the object shape.

**Representation specialization: numbers.** JavaScript has no integer type, only a Number type that is the set of 64-bit IEEE-754 floating-point numbers (“doubles”). But many JavaScript operators, in particular array accesses and bitwise operators, really operate on integers, so they first convert the number to an integer, and then convert any integer result back to a double.<sup>1</sup> Clearly, a JavaScript VM that wants to be fast must find a way to operate on integers directly and avoid these conversions.

In TraceMonkey, we support two representations for numbers: integers and doubles. The interpreter uses integer representations as much as it can, switching for results that can only be represented as doubles. When a trace is started, some values may be imported and represented as integers. Some operations on integers require guards. For example, adding two integers can produce a value too large for the integer representation.

**Function inlining.** LIR traces can cross function boundaries in either direction, achieving function inlining. Move instructions need to be recorded for function entry and exit to copy arguments in and return values out. These move statements are then optimized away by the compiler using copy propagation. In order to be able to return to the interpreter, the trace must also generate LIR to record that a call frame has been entered and exited. The frame entry and exit LIR saves just enough information to allow the interpreter call stack to be restored later and is much simpler than the interpreter’s standard call code. If the function being entered is not constant (which in JavaScript includes any call by function name), the recorder must also emit LIR to guard that the function is the same.

**Guards and side exits.** Each optimization described above requires one or more guards to verify the assumptions made in doing the optimization. A guard is just a group of LIR instructions that performs a test and conditional exit. The exit branches to a *side exit*, a small off-trace piece of LIR that returns a pointer to a structure that describes the reason for the exit along with the interpreter PC at the exit point and any other data needed to restore the interpreter’s state structures.

**Aborts.** Some constructs are difficult to record in LIR traces. For example, `eval` or calls to external functions can change the program state in unpredictable ways, making it difficult for the tracer to know the current type map in order to continue tracing. A tracing implementation can also have any number of other limitations, e.g., a small-memory device may limit the length of traces. When any situation occurs that prevents the implementation from continuing trace recording, the implementation *aborts* trace recording and returns to the trace monitor.

## 3.2 Trace Trees

Especially simple loops, namely those where control flow, value types, value representations, and inlined functions are all invariant, can be represented by a single trace. But most loops have at least some variation, and so the program will take side exits from the main trace. When a side exit becomes hot, TraceMonkey starts a new *branch trace* from that point and patches the side exit to jump directly to that trace. In this way, a single trace expands on demand to a single-entry, multiple-exit *trace tree*.

This section explains how trace trees are formed during execution. The goal is to form trace trees during execution that cover all the hot paths of the program.

**Starting a tree.** Tree trees always start at loop headers, because they are a natural place to look for hot paths. In TraceMonkey, loop headers are easy to detect—the bytecode compiler ensures that a bytecode is a loop header iff it is the target of a backward branch. TraceMonkey starts a tree when a given loop header has been executed a certain number of times (2 in the current implementation). Starting a tree just means starting recording a trace for the current point and type map and marking the trace as the root of a tree. Each tree is associated with a loop header and type map, so there may be several trees for a given loop header.

**Closing the loop.** Trace recording can end in several ways.

Ideally, the trace reaches the loop header where it started with the same type map as on entry. This is called a *type-stable* loop iteration. In this case, the end of the trace can jump right to the beginning, as all the value representations are exactly as needed to enter the trace. The jump can even skip the usual code that would copy out the state at the end of the trace and copy it back in to the trace activation record to enter a trace.

In certain cases the trace might reach the loop header with a different type map. This scenario is sometime observed for the first iteration of a loop. Some variables inside the loop might initially be *undefined*, before they are set to a concrete type during the first loop iteration. When recording such an iteration, the recorder cannot link the trace back to its own loop header since it is *type-unstable*. Instead, the iteration is terminated with a side exit that will always fail and return to the interpreter. At the same time a new trace is recorded with the new type map. Every time an additional type-unstable trace is added to a region, its exit type map is compared to the entry map of all existing traces in case they complement each other. With this approach we are able to cover type-unstable loop iterations as long they eventually form a stable equilibrium.

Finally, the trace might exit the loop before reaching the loop header, for example because execution reaches a `break` or `return` statement. In this case, the VM simply ends the trace with an exit to the trace monitor.

As mentioned previously, we may speculatively chose to represent certain Number-typed values as integers on trace. We do so when we observe that Number-typed variables contain an integer value at trace entry. If during trace recording the variable is unexpectedly assigned a non-integer value, we have to widen the type of the variable to a double. As a result, the recorded trace becomes inherently type-unstable since it starts with an integer value but ends with a double value. This represents a mis-speculation, since at trace entry we specialized the Number-typed value to an integer, assuming that at the loop edge we would again find an integer value in the variable, allowing us to close the loop. To avoid future speculative failures involving this variable, and to obtain a type-stable trace we note the fact that the variable in question as been observed to sometimes hold non-integer values in an advisory data structure which we call the “oracle”.

When compiling loops, we consult the oracle before specializing values to integers. Speculation towards integers is performed only if no adverse information is known to the oracle about that particular variable. Whenever we accidentally compile a loop that is type-unstable due to mis-speculation of a Number-typed variable, we immediately trigger the recording of a new trace, which based on the now updated oracle information will start with a double value and thus become type stable.

**Extending a tree.** Side exits lead to different paths through the loop, or paths with different types or representations. Thus, to completely cover the loop, the VM must record traces starting at all side exits. These traces are recorded much like root traces: there is a counter for each side exit, and when the counter reaches a hotness threshold, recording starts. Recording stops exactly as for the root trace, using the loop header of the root trace as the target to reach.

<sup>1</sup> Arrays are actually worse than this: if the index value is a number, it must be converted from a double to a string for the property access operator, and then to an integer internally to the array implementation.

Our implementation does not extend at all side exits. It extends only if the side exit is for a control-flow branch, and only if the side exit does not leave the loop. In particular we do not want to extend a trace tree along a path that leads to an outer loop, because we want to cover such paths in an outer tree through tree *nesting*.

### 3.3 Blacklisting

Sometimes, a program follows a path that cannot be compiled into a trace, usually because of limitations in the implementation. TraceMonkey does not currently support recording throwing and catching of arbitrary exceptions. This design trade off was chosen, because exceptions are usually rare in JavaScript. However, if a program opts to use exceptions intensively, we would suddenly incur a punishing runtime overhead if we repeatedly try to record a trace for this path and repeatedly fail to do so, since we abort tracing every time we observe an exception being thrown.

As a result, if a hot loop contains traces that always fail, the VM could potentially run much more slowly than the base interpreter: the VM repeatedly spends time trying to record traces, but is never able to run any. To avoid this problem, whenever the VM is about to start tracing, it must try to predict whether it will finish the trace.

Our prediction algorithm is based on *blacklisting* traces that have been tried and failed. When the VM fails to finish a trace starting at a given point, the VM records that a failure has occurred. The VM also sets a counter so that it will not try to record a trace starting at that point until it is passed a few more times (32 in our implementation). This *backoff* counter gives temporary conditions that prevent tracing a chance to end. For example, a loop may behave differently during startup than during its steady-state execution. After a given number of failures (2 in our implementation), the VM marks the fragment as blacklisted, which means the VM will never again start recording at that point.

After implementing this basic strategy, we observed that for small loops that get blacklisted, the system can spend a noticeable amount of time just finding the loop fragment and determining that it has been blacklisted. We now avoid that problem by patching the bytecode. We define an extra no-op bytecode that indicates a loop header. The VM calls into the trace monitor every time the interpreter executes a loop header no-op. To blacklist a fragment, we simply replace the loop header no-op with a regular no-op. Thus, the interpreter will never again even call into the trace monitor.

There is a related problem we have not yet solved, which occurs when a loop meets all of these conditions:

- The VM can form at least one root trace for the loop.
- There is at least one hot side exit for which the VM cannot complete a trace.
- The loop body is short.

In this case, the VM will repeatedly pass the loop header, search for a trace, find it, execute it, and fall back to the interpreter. With a short loop body, the overhead of finding and calling the trace is high, and causes performance to be even slower than the basic interpreter. So far, in this situation we have improved the implementation so that the VM can complete the branch trace. But it is hard to guarantee that this situation will never happen. As future work, this situation could be avoided by detecting and blacklisting loops for which the average trace call executes few bytecodes before returning to the interpreter.

## 4. Nested Trace Tree Formation

Figure 7 shows basic trace tree compilation (11) applied to a nested loop where the inner loop contains two paths. Usually, the inner loop (with header at  $i_2$ ) becomes hot first, and a trace tree is rooted at that point. For example, the first recorded trace may be a cycle

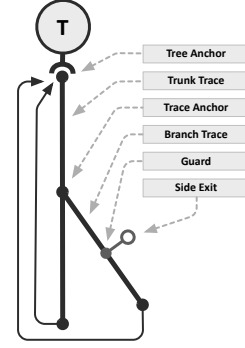


**Figure 5.** A tree with two traces, a trunk trace and one branch trace. The trunk trace contains a guard to which a branch trace was attached. The branch trace contain a guard that may fail and trigger a side exit. Both the trunk and the branch trace loop back to the tree anchor, which is the beginning of the trace tree.

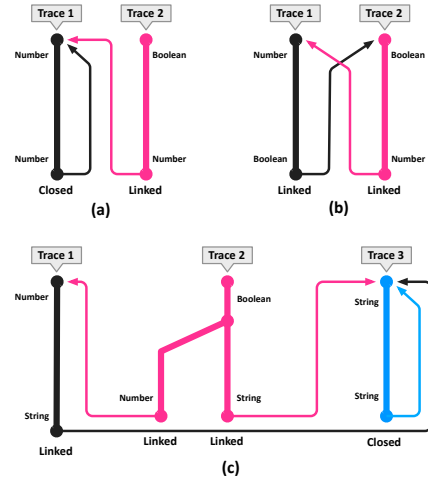


**Figure 6.** We handle type-unstable loops by allowing traces to compile that cannot loop back to themselves due to a type mismatch. As such traces accumulate, we attempt to connect their loop edges to form groups of trace trees that can execute without having to side-exit to the interpreter to cover odd type cases. This is particularly important for nested trace trees where an outer tree tries to call an inner tree (or in this case a forest of inner trees), since inner loops frequently have initially undefined values which change type to a concrete value after the first iteration.

through the inner loop,  $\{i_2, i_3, i_5, \alpha\}$ . The  $\alpha$  symbol is used to indicate that the trace loops back the tree anchor.

When execution leaves the inner loop, the basic design has two choices. First, the system can stop tracing and give up on compiling the outer loop, clearly an undesirable solution. The other choice is to continue tracing, compiling traces for the outer loop inside the inner loop's trace tree.

For example, the program might exit at  $i_5$  and record a branch trace that incorporates the outer loop:  $\{i_5, i_7, i_1, i_6, i_7, i_1, \alpha\}$ . Later, the program might take the other branch at  $i_2$  and then exit, recording another branch trace incorporating the outer loop:  $\{i_2, i_4, i_5, i_7, i_1, i_6, i_7, i_1, \alpha\}$ . Thus, the outer loop is recorded and compiled twice, and both copies must be retained in the trace cache.

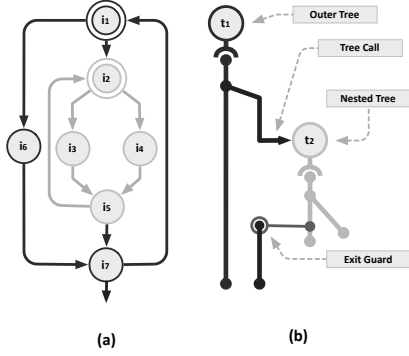


**Figure 7.** Control flow graph of a nested loop with an if statement inside the inner most loop (a). An inner tree captures the inner loop, and is nested inside an outer tree which “calls” the inner tree. The inner tree returns to the outer tree once it exits along its loop condition guard (b).

In general, if loops are nested to depth  $k$ , and each loop has  $n$  paths (on geometric average), this naïve strategy yields  $O(n^k)$  traces, which can easily fill the trace cache.

In order to execute programs with nested loops efficiently, a tracing system needs a technique for covering the nested loops with native code without exponential trace duplication.

#### 4.1 Nesting Algorithm

The key insight is that if each loop is represented by its own trace tree, the code for each loop can be contained only in its own tree, and outer loop paths will not be duplicated. Another key fact is that we are not tracing arbitrary bytecodes that might have irreducible control flow graphs, but rather bytecodes produced by a compiler for a language with structured control flow. Thus, given two loop edges, the system can easily determine whether they are nested and which is the inner loop. Using this knowledge, the system can compile inner and outer loops separately, and make the outer loop’s traces *call* the inner loop’s trace tree.

The algorithm for building nested trace trees is as follows. We start tracing at loop headers exactly as in the basic tracing system. When we exit a loop (detected by comparing the interpreter PC with the range given by the loop edge), we stop the trace. The key step of the algorithm occurs when we are recording a trace for loop  $L_R$  ( $R$  for loop being recorded) and we reach the header of a different loop  $L_O$  ( $O$  for other loop). Note that  $L_O$  must be an inner loop of  $L_R$  because we stop the trace when we exit a loop.

- If  $L_O$  has a type-matching compiled trace tree, we call  $L_O$  as a nested trace tree. If the call succeeds, then we record the call in the trace for  $L_R$ . On future executions, the trace for  $L_R$  will call the inner trace directly.
- If  $L_O$  does not have a type-matching compiled trace tree yet, we have to obtain it before we are able to proceed. In order to do this, we simply abort recording the first trace. The trace monitor will see the inner loop header, and will immediately start recording the inner loop.<sup>2</sup>

If all the loops in a nest are type-stable, then loop nesting creates no duplication. Otherwise, if loops are nested to a depth  $k$ , and each

<sup>2</sup> Instead of aborting the outer recording, we could principally merely suspend the recording, but that would require the implementation to be able to record several traces simultaneously, complicating the implementation, while saving only a few iterations in the interpreter.

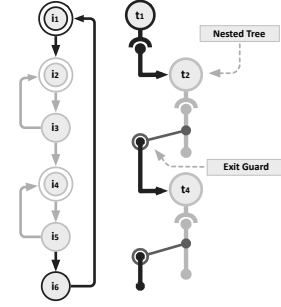


**Figure 8.** Control flow graph of a loop with two nested loops (left) and its nested trace tree configuration (right). The outer tree calls the two inner nested trace trees and places guards at their side exit locations.

loop is entered with  $m$  different type maps (on geometric average), then we compile  $O(m^k)$  copies of the innermost loop. As long as  $m$  is close to 1, the resulting trace trees will be tractable.

An important detail is that the call to the inner trace tree must act like a function call site: it must return to the same point every time. The goal of nesting is to make inner and outer loops independent; thus when the inner tree is called, it must exit to the same point in the outer tree every time with the same type map. Because we cannot actually guarantee this property, we must guard on it after the call, and side exit if the property does not hold. A common reason for the inner tree not to return to the same point would be if the inner tree took a new side exit for which it had never compiled a trace. At this point, the interpreter PC is in the inner tree, so we cannot continue recording or executing the outer tree. If this happens during recording, we abort the outer trace, to give the inner tree a chance to finish growing. A future execution of the outer tree would then be able to properly finish and record a call to the inner tree. If an inner tree side exit happens during execution of a compiled trace for the outer tree, we simply exit the outer trace and start recording a new branch in the inner tree.

#### 4.2 Blacklisting with Nesting

The blacklisting algorithm needs modification to work well with nesting. The problem is that outer loop traces often abort during startup (because the inner tree is not available or takes a side exit), which would lead to their being quickly blacklisted by the basic algorithm.

The key observation is that when an outer trace aborts because the inner tree is not ready, this is probably a temporary condition. Thus, we should not count such aborts toward blacklisting as long as we are able to build up more traces for the inner tree.

In our implementation, when an outer tree aborts on the inner tree, we increment the outer tree’s blacklist counter as usual and back off on compiling it. When the inner tree finishes a trace, we decrement the blacklist counter on the outer loop, “forgiving” the outer loop for aborting previously. We also undo the backoff so that the outer loop can start immediately trying to compile the next time we reach it.

### 5. Trace Tree Optimization

This section explains how a recorded trace is translated to an optimized machine code trace. The trace compilation subsystem, NANOJIT, is separate from the VM and can be used for other applications.



## 5.1 Optimizations

Because traces are in SSA form and have no join points or  $\phi$ -nodes, certain optimizations are easy to implement. In order to get good startup performance, the optimizations must run quickly, so we chose a small set of optimizations. We implemented the optimizations as pipelined filters so that they can be turned on and off independently, and yet all run in just two loop passes over the trace: one forward and one backward.

Every time the trace recorder emits a LIR instruction, the instruction is immediately passed to the first filter in the forward pipeline. Thus, forward filter optimizations are performed as the trace is recorded. Each filter may pass each instruction to the next filter unchanged, write a different instruction to the next filter, or write no instruction at all. For example, the constant folding filter can replace a multiply instruction like  $v_{13} := \text{mul3}, 1000$  with a constant instruction  $v_{13} = 3000$ .

We currently apply four forward filters:

- On ISAs without floating-point instructions, a soft-float filter converts floating-point LIR instructions to sequences of integer instructions.
- CSE (constant subexpression elimination),
- expression simplification, including constant folding and a few algebraic identities (e.g.,  $a - a = 0$ ), and
- source language semantic-specific expression simplification, primarily algebraic identities that allow DOUBLE to be replaced with INT. For example, LIR that converts an INT to a DOUBLE and then back again would be removed by this filter.

When trace recording is completed, nanjit runs the backward optimization filters. These are used for optimizations that require backward program analysis. When running the backward filters, nanjit reads one LIR instruction at a time, and the reads are passed through the pipeline.

We currently apply three backward filters:

- Dead data-stack store elimination. The LIR trace encodes many stores to locations in the interpreter stack. But these values are never read back before exiting the trace (by the interpreter or another trace). Thus, stores to the stack that are overwritten before the next exit are dead. Stores to locations that are off the top of the interpreter stack at future exits are also dead.
- Dead call-stack store elimination. This is the same optimization as above, except applied to the interpreter’s call stack used for function call inlining.
- Dead code elimination. This eliminates any operation that stores to a value that is never used.

After a LIR instruction is successfully read (“pulled”) from the backward filter pipeline, nanjit’s code generator emits native machine instruction(s) for it.

## 5.2 Register Allocation

We use a simple greedy register allocator that makes a single backward pass over the trace (it is integrated with the code generator). By the time the allocator has reached an instruction like  $v_3 = \text{add } v_1, v_2$ , it has already assigned a register to  $v_3$ . If  $v_1$  and  $v_2$  have not yet been assigned registers, the allocator assigns a free register to each. If there are no free registers, a value is selected for spilling. We use a class heuristic that selects the “oldest” register-carried value (6).

The heuristic considers the set  $R$  of values  $v$  in registers immediately after the current instruction for spilling. Let  $v_m$  be the last instruction before the current where each  $v$  is referred to. Then the

| Tag | JS Type                          | Description                                  |
|-----|----------------------------------|--|
| xx1 | number                           | 31-bit integer representation                |
| 000 | object                           | pointer to JSObject handle                   |
| 010 | number                           | pointer to double handle                     |
| 100 | string                           | pointer to JSString handle                   |
| 110 | boolean<br>null, or<br>undefined | enumeration for null, undefined, true, false |

**Figure 9. Tagged values in the SpiderMonkey JS interpreter.** Testing tags, unboxing (extracting the untagged value) and boxing (creating tagged values) are significant costs. Avoiding these costs is a key benefit of tracing.

heuristic selects  $v$  with minimum  $v_m$ . The motivation is that this frees up a register for as long as possible given a single spill.

If we need to spill a value  $v_s$  at this point, we generate the restore code just after the code for the current instruction. The corresponding spill code is generated just after the last point where  $v_s$  was used. The register that was assigned to  $v_s$  is marked free for the preceding code, because that register can now be used freely without affecting the following code.

## 6. Implementation

To demonstrate the effectiveness of our approach, we have implemented a trace-based dynamic compiler for the SpiderMonkey JavaScript Virtual Machine (4). SpiderMonkey is the JavaScript VM embedded in Mozilla’s Firefox open-source web browser (2), which is used by more than 200 million users world-wide. The core of SpiderMonkey is a bytecode interpreter implemented in C++.

In SpiderMonkey, all JavaScript values are represented by the type `jsval`. A `jsval` is machine word in which up to the 3 of the least significant bits are a type tag, and the remaining bits are data. See Figure 6 for details. All pointers contained in `jsvals` point to GC-controlled blocks aligned on 8-byte boundaries.

JavaScript *object* values are mappings of string-valued property names to arbitrary values. They are represented in one of two ways in SpiderMonkey. Most objects are represented by a shared structural description, called the *object shape*, that maps property names to array indexes using a hash table. The object stores a pointer to the shape and the array of its own property values. Objects with large, unique sets of property names store their properties directly in a hash table.

The garbage collector is an exact, non-generational, stop-the-world mark-and-sweep collector.

In the rest of this section we discuss key areas of the TraceMonkey implementation.

### 6.1 Calling Compiled Traces

Compiled traces are stored in a *trace cache*, indexed by interpreter PC and type map. Traces are compiled so that they may be called as functions using standard native calling conventions (e.g., FASTCALL on x86).

The interpreter must hit a loop edge and enter the monitor in order to call a native trace for the first time. The monitor computes the current type map, checks the trace cache for a trace for the current PC and type map, and if it finds one, executes the trace.

To execute a trace, the monitor must build a trace activation record containing imported local and global variables, temporary stack space, and space for arguments to native calls. The local and global values are then copied from the interpreter state to the trace activation record. Then, the trace is called like a normal C function pointer.

When a trace call returns, the monitor restores the interpreter state. First, the monitor checks the reason for the trace exit and applies blacklisting if needed. Then, it pops or synthesizes interpreter JavaScript call stack frames as needed. Finally, it copies the imported variables back from the trace activation record to the interpreter state.

At least in the current implementation, these steps have a non-negligible runtime cost, so minimizing the number of interpreter-to-trace and trace-to-interpreter transitions is essential for performance. (see also Section 3.3). Our experiments (see Figure 12) show that for programs we can trace well such transitions happen infrequently and hence do not contribute significantly to total runtime. In a few programs, where the system is prevented from recording branch traces for hot side exits by aborts, this cost can rise to up to 10% of total execution time.

## 6.2 Trace Stitching

Transitions from a trace to a branch trace at a side exit avoid the costs of calling traces from the monitor, in a feature called *trace stitching*. At a side exit, the exiting trace only needs to write live register-carried values back to its trace activation record. In our implementation, identical type maps yield identical activation record layouts, so the trace activation record can be reused immediately by the branch trace.

In programs with branchy trace trees with small traces, trace stitching has a noticeable cost. Although writing to memory and then soon reading back would be expected to have a high L1 cache hit rate, for small traces the increased instruction count has a noticeable cost. Also, if the writes and reads are very close in the dynamic instruction stream, we have found that current x86 processors often incur penalties of 6 cycles or more (e.g., if the instructions use different base registers with equal values, the processor may not be able to detect that the addresses are the same right away).

The alternate solution is to recompile an entire trace tree, thus achieving inter-trace register allocation (10). The disadvantage is that tree recompilation takes time quadratic in the number of traces. We believe that the cost of recompiling a trace tree every time a branch is added would be prohibitive. That problem might be mitigated by recompiling only at certain points, or only for very hot, stable trees.

In the future, multicore hardware is expected to be common, making background tree recompilation attractive. In a closely related project (13) background recompilation yielded speedups of up to 1.25x on benchmarks with many branch traces. We plan to apply this technique to TraceMonkey as future work.

## 6.3 Trace Recording

The job of the trace recorder is to emit LIR with identical semantics to the currently running interpreter bytecode trace. A good implementation should have low impact on non-tracing interpreter performance and a convenient way for implementers to maintain semantic equivalence.

In our implementation, the only direct modification to the interpreter is a call to the trace monitor at loop edges. In our benchmark results (see Figure 12) the total time spent in the monitor (for all activities) is usually less than 5%, so we consider the interpreter impact requirement met. Incrementing the loop hit counter is expensive because it requires us to look up the loop in the trace cache, but we have tuned our loops to become hot and trace very quickly (on the second iteration). The hit counter implementation could be improved, which might give us a small increase in overall performance, as well as more flexibility with tuning hotness thresholds. Once a loop is blacklisted we never call into the trace monitor for that loop (see Section 3.3).

Recording is activated by a pointer swap that sets the interpreter’s dispatch table to call a single “interrupt” routine for every bytecode. The interrupt routine first calls a bytecode-specific recording routine. Then, it turns off recording if necessary (e.g., the trace ended). Finally, it jumps to the standard interpreter bytecode implementation. Some bytecodes have effects on the type map that cannot be predicted before executing the bytecode (e.g., calling `String.charCodeAt`, which returns an integer or `NaN` if the index argument is out of range). For these, we arrange for the interpreter to call into the recorder again after executing the bytecode. Since such hooks are relatively rare, we embed them directly into the interpreter, with an additional runtime check to see whether a recorder is currently active.

While separating the interpreter from the recorder reduces individual code complexity, it also requires careful implementation and extensive testing to achieve semantic equivalence.

In some cases achieving this equivalence is difficult since SpiderMonkey follows a *fat-bytecode* design, which was found to be beneficial to pure interpreter performance.

In fat-bytecode designs, individual bytecodes can implement complex processing (e.g., the `getprop` bytecode, which implements full JavaScript property value access, including special cases for cached and dense array access).

Fat bytecodes have two advantages: fewer bytecodes means lower dispatch cost, and bigger bytecode implementations give the compiler more opportunities to optimize the interpreter.

Fat bytecodes are a problem for TraceMonkey because they require the recorder to reimplement the same special case logic in the same way. Also, the advantages are reduced because (a) dispatch costs are eliminated entirely in compiled traces, (b) the traces contain only one special case, not the interpreter’s large chunk of code, and (c) TraceMonkey spends less time running the base interpreter.

One way we have mitigated these problems is by implementing certain complex bytecodes in the recorder as sequences of simple bytecodes. Expressing the original semantics this way is not too difficult, and recording simple bytecodes is much easier. This enables us to retain the advantages of fat bytecodes while avoiding some of their problems for trace recording. This is particularly effective for fat bytecodes that recurse back into the interpreter, for example to convert an object into a primitive value by invoking a well-known method on the object, since it lets us inline this function call.

It is important to note that we split fat opcodes into thinner opcodes only during recording. When running purely interpretatively (i.e. code that has been blacklisted), the interpreter directly and efficiently executes the fat opcodes.

## 6.4 Preemption

SpiderMonkey, like many VMs, needs to preempt the user program periodically. The main reasons are to prevent infinitely looping scripts from locking up the host system and to schedule GC.

In the interpreter, this had been implemented by setting a “preempt now” flag that was checked on every backward jump. This strategy carried over into TraceMonkey: the VM inserts a guard on the preemption flag at every loop edge. We measured less than a 1% increase in runtime on most benchmarks for this extra guard. In practice, the cost is detectable only for programs with very short loops.

We tested and rejected a solution that avoided the guards by compiling the loop edge as an unconditional jump, and patching the jump target to an exit routine when preemption is required. This solution can make the normal case slightly faster, but then preemption becomes very slow. The implementation was also very complex, especially trying to restart execution after the preemption.

## 6.5 Calling External Functions

Like most interpreters, SpiderMonkey has a foreign function interface (FFI) that allows it to call C builtins and host system functions (e.g., web browser control and DOM access). The FFI has a standard signature for JS-callable functions, the key argument of which is an array of boxed values. External functions called through the FFI interact with the program state through an interpreter API (e.g., to read a property from an argument). There are also certain interpreter builtins that do not use the FFI, but interact with the program state in the same way, such as the `CallIteratorNext` function used with iterator objects. TraceMonkey must support this FFI in order to speed up code that interacts with the host system inside hot loops.

Calling external functions from TraceMonkey is potentially difficult because traces do not update the interpreter state until exiting. In particular, external functions may need the call stack or the global variables, but they may be out of date.

For the out-of-date call stack problem, we refactored some of the interpreter API implementation functions to re-materialize the interpreter call stack on demand.

We developed a C++ static analysis and annotated some interpreter functions in order to verify that the call stack is refreshed at any point it needs to be used. In order to access the call stack, a function must be annotated as either `FORCESSTACK` or `REQUIRESSTACK`. These annotations are also required in order to call `REQUIRESSTACK` functions, which are presumed to access the call stack transitively. `FORCESSTACK` is a trusted annotation, applied to only 5 functions, that means the function refreshes the call stack. `REQUIRESSTACK` is an untrusted annotation that means the function may only be called if the call stack has already been refreshed.

Similarly, we detect when host functions attempt to directly read or write global variables, and force the currently running trace to side exit. This is necessary since we cache and unbox global variables into the activation record during trace execution.

Since both call-stack access and global variable access are rarely performed by host functions, performance is not significantly affected by these safety mechanisms.

Another problem is that external functions can reenter the interpreter by calling scripts, which in turn again might want to access the call stack or global variables. To address this problem, we made the VM set a flag whenever the interpreter is reentered while a compiled trace is running.

Every call to an external function then checks this flag and exits the trace immediately after returning from the external function call if it is set. There are many external functions that seldom or never reenter, and they can be called without problem, and will cause trace exit only if necessary.

The FFI's boxed value array requirement has a performance cost, so we defined a new FFI that allows C functions to be annotated with their argument types so that the tracer can call them directly, without unnecessary argument conversions.

Currently, we do not support calling native property get and set override functions or DOM functions directly from trace. Support is planned future work.

## 6.6 Correctness

During development, we had access to existing JavaScript test suites, but most of them were not designed with tracing VMs in mind and contained few loops.

One tool that helped us greatly was Mozilla's JavaScript fuzz tester, JSFUNFUZZ, which generates random JavaScript programs by nesting random language elements. We modified JSFUNFUZZ to generate loops, and also to test more heavily certain constructs we suspected would reveal flaws in our implementation. For example, we suspected bugs in TraceMonkey's handling of type-unstable

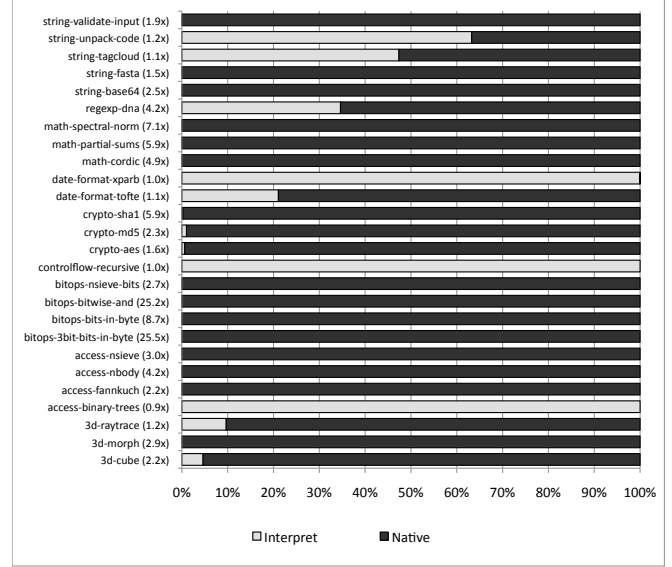


**Figure 11. Fraction of dynamic bytecodes executed by interpreter and on native traces.** The speedup vs. interpreter is shown in parentheses next to each test. The fraction of bytecodes executed while recording is too small to see in this figure, except for `crypto-md5`, where fully 3% of bytecodes are executed while recording. In most of the tests, almost all the bytecodes are executed by compiled traces. Three of the benchmarks are not traced at all and run in the interpreter.

loops and heavily branching code, and a specialized fuzz tester indeed revealed several regressions which we subsequently corrected.

## 7. Evaluation

We evaluated our JavaScript tracing implementation using SunSpider, the industry standard JavaScript benchmark suite. SunSpider consists of 26 short-running (less than 250ms, average 26ms) JavaScript programs. This is in stark contrast to benchmark suites such as SpecJVM98 (3) used to evaluate desktop and server Java VMs. Many programs in those benchmarks use large data sets and execute for minutes. The SunSpider programs carry out a variety of tasks, primarily 3d rendering, bit-bashing, cryptographic encoding, math kernels, and string processing.

All experiments were performed on a MacBook Pro with 2.2 GHz Core 2 processor and 2 GB RAM running MacOS 10.5.

**Benchmark results.** The main question is whether programs run faster with tracing. For this, we ran the standard SunSpider test driver, which starts a JavaScript interpreter, loads and runs each program once for warmup, then loads and runs each program 10 times and reports the average time taken by each. We ran 4 different configurations for comparison: (a) SpiderMonkey, the baseline interpreter, (b) TraceMonkey, (d) SquirrelFish Extreme (SFX), the call-threaded JavaScript interpreter used in Apple's WebKit, and (e) V8, the method-compiling JavaScript VM from Google.

Figure 10 shows the relative speedups achieved by tracing, SFX, and V8 against the baseline (SpiderMonkey). Tracing achieves the best speedups in integer-heavy benchmarks, up to the 25x speedup on `bitops-bitwise-and`.

TraceMonkey is the fastest VM on 9 of the 26 benchmarks (`3d-morph`, `bitops-3bit-bits-in-byte`, `bitops-bitwise-and`, `crypto-sha1`, `math-cordic`, `math-partial-sums`, `math-spectral-norm`, `string-base64`, `string-validate-input`).

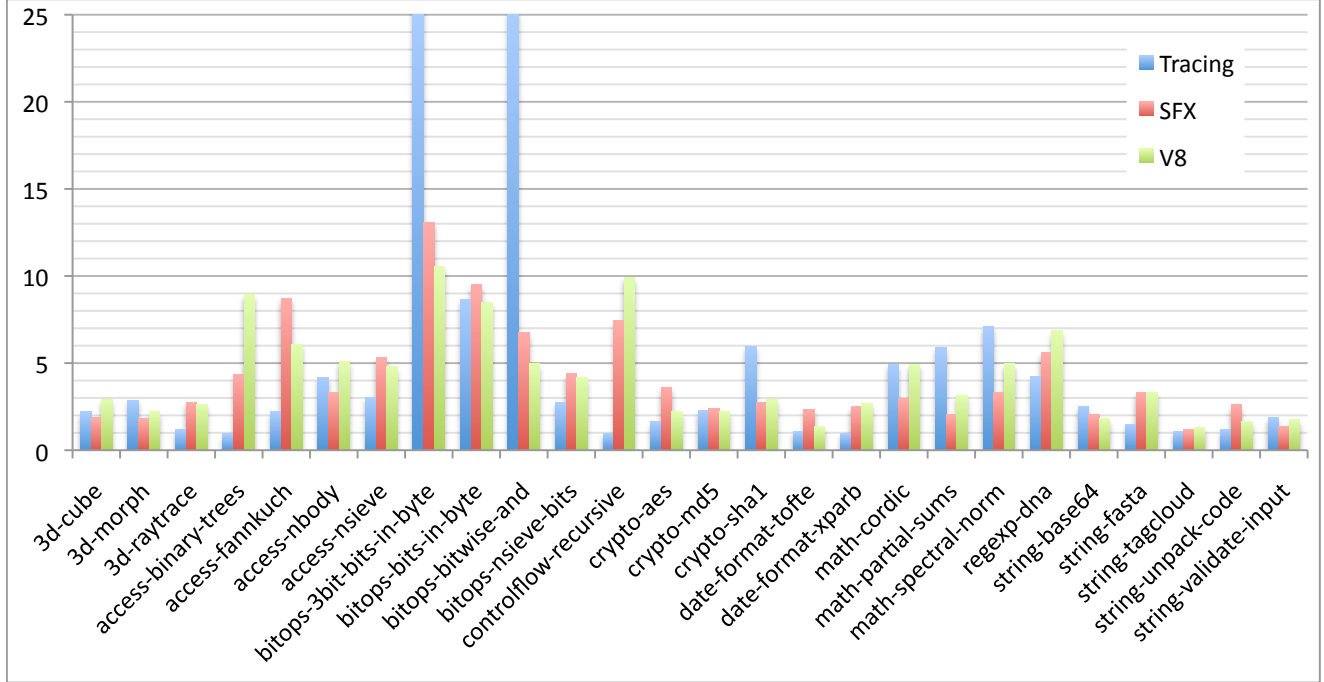


**Figure 10.** Speedup vs. a baseline JavaScript interpreter (SpiderMonkey) for our trace-based JIT compiler, Apple’s SquirrelFish Extreme inline threading interpreter and Google’s V8 JS compiler. Our system generates particularly efficient code for programs that benefit most from type specialization, which includes SunSpider Benchmark programs that perform bit manipulation. We type-specialize the code in question to use integer arithmetic, which substantially improves performance. For one of the benchmark programs we execute 25 times faster than the SpiderMonkey interpreter, and almost 5 times faster than V8 and SFX. For a large number of benchmarks all three VMs produce similar results. We perform worst on benchmark programs that we do not trace and instead fall back onto the interpreter. This includes the recursive benchmarks `access-binary-trees` and `control-flow-recursive`, for which we currently don’t generate any native code.

In particular, the `bitops` benchmarks are short programs that perform many bitwise operations, so TraceMonkey can cover the entire program with 1 or 2 traces that operate on integers. TraceMonkey runs all the other programs in this set almost entirely as native code.

`regexp-dna` is dominated by regular expression matching, which is implemented in all 3 VMs by a special regular expression compiler. Thus, performance on this benchmark has little relation to the trace compilation approach discussed in this paper.

TraceMonkey’s smaller speedups on the other benchmarks can be attributed to a few specific causes:

- The implementation does not currently trace recursion, so TraceMonkey achieves a small speedup or no speedup on benchmarks that use recursion extensively: `3d-cube`, `3d-raytrace`, `access-binary-trees`, `string-tagcloud`, and `controlflow-recursive`.
- The implementation does not currently trace `eval` and some other functions implemented in C. Because `date-format-tofte` and `date-format-xparb` use such functions in their main loops, we do not trace them.
- The implementation does not currently trace through regular expression `replace` operations. The `replace` function can be passed a function object used to compute the replacement text. Our implementation currently does not trace functions called as `replace` functions. The run time of `string-unpack-code` is dominated by such a `replace` call.

- Two programs trace well, but have a long compilation time. `access-nbody` forms a large number of traces (81). `crypto-md5` forms one very long trace. We expect to improve performance on this programs by improving the compilation speed of nanojit.
- Some programs trace very well, and speed up compared to the interpreter, but are not as fast as SFX and/or V8, namely `bitops-bits-in-byte`, `bitops-nsieve-bits`, `access-fannkuch`, `access-nsieve`, and `crypto-aes`. The reason is not clear, but all of these programs have nested loops with small bodies, so we suspect that the implementation has a relatively high cost for calling nested traces. `string-fast` traces well, but its run time is dominated by string processing builtins, which are unaffected by tracing and seem to be less efficient in SpiderMonkey than in the two other VMs.

**Detailed performance metrics.** In Figure 11 we show the fraction of instructions interpreted and the fraction of instructions executed as native code. This figure shows that for many programs, we are able to execute almost all the code natively.

Figure 12 breaks down the total execution time into four activities: interpreting bytecodes while not recording, recording traces (including time taken to interpret the recorded trace), compiling traces to native code, and executing native code traces.

These detailed metrics allow us to estimate parameters for a simple model of tracing performance. These estimates should be considered very rough, as the values observed on the individual benchmarks have large standard deviations (on the order of the



|                          | Loops | Trees | Traces | Aborts | Flushes | Trees/Loop | Traces/Tree | Traces/Loop | Speedup |
|--------------------------|-------|-------|--------|--------|---------|------------|-------------|-------------|---------|
| 3d-cube                  | 25    | 27    | 29     | 3      | 0       | 1.1        | 1.1         | 1.2         | 2.20x   |
| 3d-morph                 | 5     | 8     | 8      | 2      | 0       | 1.6        | 1.0         | 1.6         | 2.86x   |
| 3d-raytrace              | 10    | 25    | 100    | 10     | 1       | 2.5        | 4.0         | 10.0        | 1.18x   |
| access-binary-trees      | 0     | 0     | 0      | 5      | 0       | -          | -           | -           | 0.93x   |
| access-fannkuch          | 10    | 34    | 57     | 24     | 0       | 3.4        | 1.7         | 5.7         | 2.20x   |
| access-nbody             | 8     | 16    | 18     | 5      | 0       | 2.0        | 1.1         | 2.3         | 4.19x   |
| access-nsieve            | 3     | 6     | 8      | 3      | 0       | 2.0        | 1.3         | 2.7         | 3.05x   |
| bitops-3bit-bits-in-byte | 2     | 2     | 2      | 0      | 0       | 1.0        | 1.0         | 1.0         | 25.47x  |
| bitops-bits-in-byte      | 3     | 3     | 4      | 1      | 0       | 1.0        | 1.3         | 1.3         | 8.67x   |
| bitops-bitwise-and       | 1     | 1     | 1      | 0      | 0       | 1.0        | 1.0         | 1.0         | 25.20x  |
| bitops-nsieve-bits       | 3     | 3     | 5      | 0      | 0       | 1.0        | 1.7         | 1.7         | 2.75x   |
| controlflow-recursive    | 0     | 0     | 0      | 1      | 0       | -          | -           | -           | 0.98x   |
| crypto-aes               | 50    | 72    | 78     | 19     | 0       | 1.4        | 1.1         | 1.6         | 1.64x   |
| crypto-md5               | 4     | 4     | 5      | 0      | 0       | 1.0        | 1.3         | 1.3         | 2.30x   |
| crypto-sha1              | 5     | 5     | 10     | 0      | 0       | 1.0        | 2.0         | 2.0         | 5.95x   |
| date-format-tofte        | 3     | 3     | 4      | 7      | 0       | 1.0        | 1.3         | 1.3         | 1.07x   |
| date-format-xparb        | 3     | 3     | 11     | 3      | 0       | 1.0        | 3.7         | 3.7         | 0.98x   |
| math-cordic              | 2     | 4     | 5      | 1      | 0       | 2.0        | 1.3         | 2.5         | 4.92x   |
| math-partial-sums        | 2     | 4     | 4      | 1      | 0       | 2.0        | 1.0         | 2.0         | 5.90x   |
| math-spectral-norm       | 15    | 20    | 20     | 0      | 0       | 1.3        | 1.0         | 1.3         | 7.12x   |
| regexp-dna               | 2     | 2     | 2      | 0      | 0       | 1.0        | 1.0         | 1.0         | 4.21x   |
| string-base64            | 3     | 5     | 7      | 0      | 0       | 1.7        | 1.4         | 2.3         | 2.53x   |
| string-fasta             | 5     | 11    | 15     | 6      | 0       | 2.2        | 1.4         | 3.0         | 1.49x   |
| string-tagcloud          | 3     | 6     | 6      | 5      | 0       | 2.0        | 1.0         | 2.0         | 1.09x   |
| string-unpack-code       | 4     | 4     | 37     | 0      | 0       | 1.0        | 9.3         | 9.3         | 1.20x   |
| string-validate-input    | 6     | 10    | 13     | 1      | 0       | 1.7        | 1.3         | 2.2         | 1.86x   |

**Figure 13.** Detailed trace recording statistics for the SunSpider benchmark set.

mean). We exclude `regexp-dna` from the following calculations, because most of its time is spent in the regular expression matcher, which has much different performance characteristics from the other programs. (Note that this only makes a difference of about 10% in the results.) Dividing the total execution time in processor clock cycles by the number of bytecodes executed in the base interpreter shows that on average, a bytecode executes in about 35 cycles. Native traces take about 9 cycles per bytecode, a 3.9x speedup over the interpreter.

Using similar computations, we find that trace recording takes about 3800 cycles per bytecode, and compilation 3150 cycles per bytecode. Hence, during recording and compiling the VM runs at 1/200 the speed of the interpreter. Because it costs 6950 cycles to compile a bytecode, and we save 26 cycles each time that code is run natively, we break even after running a trace 270 times.

The other VMs we compared with achieve an overall speedup of 3.0x relative to our baseline interpreter. Our estimated native code speedup of 3.9x is significantly better. This suggests that our compilation techniques can generate more efficient native code than any other current JavaScript VM.

These estimates also indicate that our startup performance could be substantially better if we improved the speed of trace recording and compilation. The estimated 200x slowdown for recording and compilation is very rough, and may be influenced by startup factors in the interpreter (e.g., caches that have not warmed up yet during recording). One observation supporting this conjecture is that in the tracer, interpreted bytecodes take about 180 cycles to run. Still, recording and compilation are clearly both expensive, and a better implementation, possibly including redesign of the LIR abstract syntax or encoding, would improve startup performance.

Our performance results confirm that type specialization using trace trees substantially improves performance. We are able to outperform the fastest available JavaScript compiler (V8) and the

fastest available JavaScript inline threaded interpreter (SFX) on 9 of 26 benchmarks.

## 8. Related Work

**Trace optimization for dynamic languages.** The closest area of related work is on applying trace optimization to type-specialize dynamic languages. Existing work shares the idea of generating type-specialized code speculatively with guards along interpreter traces.

To our knowledge, Rigo’s Psycho (16) is the only published type-specializing trace compiler for a dynamic language (Python). Psycho does not attempt to identify hot loops or inline function calls. Instead, Psycho transforms loops to mutual recursion before running and traces all operations.

Pall’s LuaJIT is a Lua VM in development that uses trace compilation ideas. (1). There are no publications on LuaJIT but the creator has told us that LuaJIT has a similar design to our system, but will use a less aggressive type speculation (e.g., using a floating-point representation for all number values) and does not generate nested traces for nested loops.

**General trace optimization.** General trace optimization has a longer history that has treated mostly native code and typed languages like Java. Thus, these systems have focused less on type specialization and more on other optimizations.

Dynamo (7) by Bala et al, introduced native code tracing as a replacement for profile-guided optimization (PGO). A major goal was to perform PGO online so that the profile was specific to the current execution. Dynamo used loop headers as candidate hot traces, but did not try to create loop traces specifically.

Trace trees were originally proposed by Gal et al. (11) in the context of Java, a statically typed language. Their trace trees actually inlined parts of outer loops within the inner loops (because

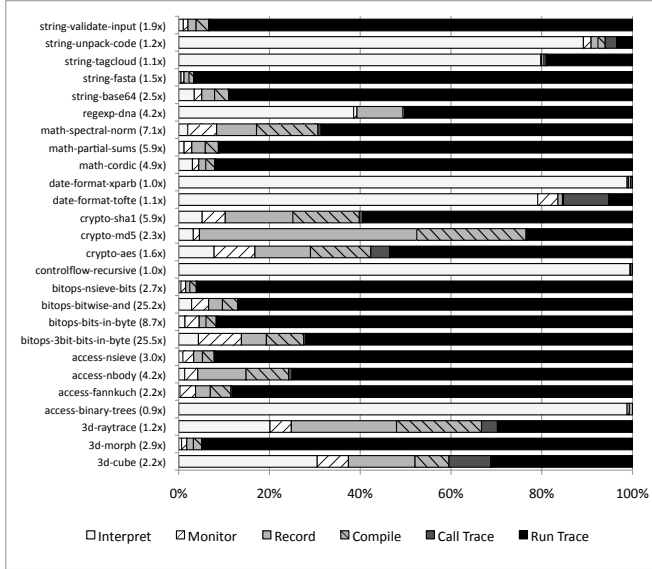


**Figure 12. Fraction of time spent on major VM activities.** The speedup vs. interpreter is shown in parentheses next to each test. Most programs where the VM spends the majority of its time running native code have a good speedup. Recording and compilation costs can be substantial; speeding up those parts of the implementation would improve SunSpider performance.

inner loops become hot first), leading to much greater tail duplication.

YETI, from Zaleski et al. (19) applied Dynamo-style tracing to Java in order to achieve inlining, indirect jump elimination, and other optimizations. Their primary focus was on designing an interpreter that could easily be gradually re-engineered as a tracing VM.

Suganuma et al. (18) described region-based compilation (RBC), a relative of tracing. A region is an subprogram worth optimizing that can include subsets of any number of methods. Thus, the compiler has more flexibility and can potentially generate better code, but the profiling and compilation systems are correspondingly more complex.

**Type specialization for dynamic languages.** Dynamic language implementors have long recognized the importance of type specialization for performance. Most previous work has focused on methods instead of traces.

Chambers et. al (9) pioneered the idea of compiling multiple versions of a procedure specialized for the input types in the language Self. In one implementation, they generated a specialized method online each time a method was called with new input types. In another, they used an offline whole-program static analysis to infer input types and constant receiver types at call sites. Interestingly, the two techniques produced nearly the same performance.

Salib (17) designed a type inference algorithm for Python based on the Cartesian Product Algorithm and used the results to specialize on types and translate the program to C++.

McCloskey (14) has work in progress based on a language-independent type inference that is used to generate efficient C implementations of JavaScript and Python programs.

**Native code generation by interpreters.** The traditional interpreter design is a virtual machine that directly executes ASTs or machine-code-like bytecodes. Researchers have shown how to gen-

erate native code with nearly the same structure but better performance.

Call threading, also known as context threading (8), compiles methods by generating a native call instruction to an interpreter method for each interpreter bytecode. A call-return pair has been shown to be a potentially much more efficient dispatch mechanism than the indirect jumps used in standard bytecode interpreters.

Inline threading (15) copies chunks of interpreter native code which implement the required bytecodes into a native code cache, thus acting as a simple per-method JIT compiler that eliminates the dispatch overhead.

Neither call threading nor inline threading perform type specialization.

Apple’s SquirrelFish Extreme (5) is a JavaScript implementation based on call threading with selective inline threading. Combined with efficient interpreter engineering, these threading techniques have given SFX excellent performance on the standard SunSpider benchmarks.

Google’s V8 is a JavaScript implementation primarily based on inline threading, with call threading only for very complex operations.

## 9. Conclusions

This paper described how to run dynamic languages efficiently by recording hot traces and generating type-specialized native code. Our technique focuses on aggressively inlined loops, and for each loop, it generates a tree of native code traces representing the paths and value types through the loop observed at run time. We explained how to identify loop nesting relationships and generate nested traces in order to avoid excessive code duplication due to the many paths through a loop nest. We described our type specialization algorithm. We also described our trace compiler, which translates a trace from an intermediate representation to optimized native code in two linear passes.

Our experimental results show that in practice loops typically are entered with only a few different combinations of value types of variables. Thus, a small number of traces per loop is sufficient to run a program efficiently. Our experiments also show that on programs amenable to tracing, we achieve speedups of 2x to 20x.

## 10. Future Work

Work is underway in a number of areas to further improve the performance of our trace-based JavaScript compiler. We currently do not trace across recursive function calls, but plan to add the support for this capability in the near term. We are also exploring adoption of the existing work on tree recompilation in the context of the presented dynamic compiler in order to minimize JIT pause times and obtain the best of both worlds, fast tree stitching as well as the improved code quality due to tree recompilation.

We also plan on adding support for tracing across regular expression substitutions using lambda functions, function applications and expression evaluation using `eval`. All these language constructs are currently executed via interpretation, which limits our performance for applications that use those features.

## Acknowledgments

Parts of this effort have been sponsored by the National Science Foundation under grants CNS-0615443 and CNS-0627747, as well as by the California MICRO Program and industrial sponsor Sun Microsystems under Project No. 07-127.

The U.S. Government is authorized to reproduce and distribute reprints for Governmental purposes notwithstanding any copyright annotation thereon. Any opinions, findings, and conclusions or recommendations expressed here are those of the author and should

not be interpreted as necessarily representing the official views, policies or endorsements, either expressed or implied, of the National Science foundation (NSF), any other agency of the U.S. Government, or any of the companies mentioned above.

## References

- [1] LuaJIT roadmap 2008 - <http://lua-users.org/lists/lua-l/2008-02/msg00051.html>.
- [2] Mozilla — Firefox web browser and Thunderbird email client - <http://www.mozilla.com>.
- [3] SPECJVM98 - <http://www.spec.org/jvm98/>.
- [4] SpiderMonkey (JavaScript-C) Engine - <http://www.mozilla.org/js/spidermonkey/>.
- [5] Surfin' Safari - Blog Archive - Announcing SquirrelFish Extreme - <http://webkit.org/blog/214/introducing-squirrelfish-extreme/>.
- [6] A. Aho, R. Sethi, J. Ullman, and M. Lam. Compilers: Principles, techniques, and tools, 2006.
- [7] V. Bala, E. Duesterwald, and S. Banerjia. Dynamo: A transparent dynamic optimization system. In *Proceedings of the ACM SIGPLAN Conference on Programming Language Design and Implementation*, pages 1–12. ACM Press, 2000.
- [8] M. Berndt, B. Vitale, M. Zaleski, and A. Brown. Context Threading: a Flexible and Efficient Dispatch Technique for Virtual Machine Interpreters. In *Code Generation and Optimization, 2005. CGO 2005. International Symposium on*, pages 15–26, 2005.
- [9] C. Chambers and D. Ungar. Customization: Optimizing Compiler Technology for SELF, a Dynamically-Typed Object-Oriented Programming Language. In *Proceedings of the ACM SIGPLAN 1989 Conference on Programming Language Design and Implementation*, pages 146–160. ACM New York, NY, USA, 1989.
- [10] A. Gal. *Efficient Bytecode Verification and Compilation in a Virtual Machine Dissertation*. PhD thesis, University Of California, Irvine, 2006.
- [11] A. Gal, C. W. Probst, and M. Franz. HotpathVM: An effective JIT compiler for resource-constrained devices. In *Proceedings of the International Conference on Virtual Execution Environments*, pages 144–153. ACM Press, 2006.
- [12] C. Garrett, J. Dean, D. Grove, and C. Chambers. Measurement and Application of Dynamic Receiver Class Distributions. 1994.
- [13] J. Ha, M. R. Haghighat, S. Cong, and K. S. McKinley. A concurrent trace-based just-in-time compiler for javascript. Dept. of Computer Sciences, The University of Texas at Austin, TR-09-06, 2009.
- [14] B. McCloskey. Personal communication.
- [15] I. Piumarta and F. Ricciardi. Optimizing direct threaded code by selective inlining. In *Proceedings of the ACM SIGPLAN 1998 conference on Programming language design and implementation*, pages 291–300. ACM New York, NY, USA, 1998.
- [16] A. Rigo. Representation-Based Just-In-time Specialization and the Psyco Prototype for Python. In *PEPM*, 2004.
- [17] M. Salib. Starkiller: A Static Type Inferencer and Compiler for Python. In *Master's Thesis*, 2004.
- [18] T. Suganuma, T. Yasue, and T. Nakatani. A Region-Based Compilation Technique for Dynamic Compilers. *ACM Transactions on Programming Languages and Systems (TOPLAS)*, 28(1):134–174, 2006.
- [19] M. Zaleski, A. D. Brown, and K. Stoodley. YETI: A gradually Extensible Trace Interpreter. In *Proceedings of the International Conference on Virtual Execution Environments*, pages 83–93. ACM Press, 2007.